Energy & Buildings 296 (2023) 113368

Contents lists available at ScienceDirect

Energy & Buildings

journal homepage: www.elsevier.com/locate/enb

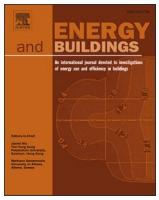

A multistep approach for the hygrothermal assessment of a hybrid timber and aluminium based facade system exposed to different sub-climates in Norway

Guilherme B.A. Coelho *, Dimitrios Kraniotis

Department of Built Environment, Faculty of Technology, Art and Design, Oslo Metropolitan University, PO box 4 St. Olavs plass, Oslo NO-0130, Norway

ARTICLE INFO

Keywords:
Hybrid facade system
Building energy simulation, BES
Heat, air and moisture transport, HAM
Weather data
Data gap filling
Climate change
Mould growth
Numerical simulation
Hygrothermal performance

ABSTRACT

This paper describes a multistep approach that allows the design and assessment a hybrid, timber-based, facade system that can withstand current real conditions without being prone to mould. This approach is aligned with today's drive for a more sustainable built environment. A typical office building with the hybrid system was simulated in a BES tool to obtain the indoor conditions in three selected locations in Norway. Historic measured weather data were used to build climate files, in accordance with ISO 15927-4 methodology. The global radiation was split using the DIRINT model, while a user-independent code was developed to find and fill the weather datasets gaps. A model was built using a one-dimensional HAM software for each facade section to assess its hygrothermal performance, whose studies are scarce in literature, and determine whether the system is appropriate for Nordic climate. This analysis included mould growth risk assessment, determining the variance of the transient U-values and the influence of the wood surface treatment on the drying capacity of the facade. The obtained energy consumptions are in accordance with the current Norwegian regulations. Under normal conditions, the system works properly. However, problems arise if a higher initial moisture content exists in the materials.

1. Introduction

Due to today's sustainability concerns, we must find ways to decrease the CO_2 footprint of materials and systems in buildings, considering their whole life cycle. This is largely due to the fact that buildings are responsible for 40 % of the total energy consumption in Europe [1], which means that they are responsible for a large slice of the greenhouse gases emissions (GHGs) during the buildings operation phase. In addition, buildings are responsible for large amount of embodied GHG emissions, i.e., during material production and transportation, construction etc. In sum, they correspond to 35 % of the total GHGs emissions – i.e. ca 1,500,000,000 tonnes of eq-CO_2 in 2017 [2], with Europe being the third most GHGs emitting region of the world [2].

The *StaticusCare project* [3], financed by EEA/Norway Grants, emerged from this need, since it aims to decrease the GHG emissions associated to the construction industry by developing a hybrid, timber and aluminium, unitized based facade system that will integrate IoT sensors. These sensors will be part of a predictive building maintenance system [3]. A decrease of the facade's carbon dioxide (CO_2) footprint of 70–75 % and also of the non-renewable energy consumption to 53–56 % [3] is expected when compared with Staticus, which is a facade design and building specialized company that is responsible for this R&D project, traditional solely aluminium facade frame system.

A great advantage of a hybrid system is that the final product performance can be maximized by the benefits of its constituents parts [4]. The inclusion of the timber in the facade system has a clearer positive effect at several levels. Firstly, wood and, consequently, timber, are environmentally friendly since wood is a renewable resource and a carbon neutral material that stores CO_2 [4], while a great amount of energy has to be spent to produce aluminium [5]. Secondly, timber has good mechanical properties, but it is not a material that has a ductile behaviour, which is of key importance for man-made constructions. Therefore, it is necessary to couple timber with ductile materials so that the hybrid product has a ductile behaviour [4]. Thirdly, timber is also known for its good thermal and acoustic insulation capability [4,6], as well as its capacity to buffer the maxima and minima of indoor humidity [7] and reduce conductive heat losses [8,9] due to its hygroscopic nature [10], and not least for its good aesthetic and workability [11].

* Corresponding author.
E-mail address: coelho@oslomet.no (G.B.A. Coelho).

https://doi.org/10.1016/j.enbuild.2023.113368
Received 1 May 2023; Received in revised form 29 June 2023; Accepted 12 July 2023
Available online 17 July 2023

The quickness within which a unitized facade can be installed is also a great advantage [12], since the factory pre-prepared facade units can be installed straight from their transportation trucks [12]. This fast-installing capacity has the advantage of protecting the inside of the building from outdoor damaging sources, e.g. rain [12], which is essential so that there is no entrapped moisture. The prefabrication nature of this type of system has even the advantage of enabling the use of timber-based systems in locations that wood and its derivates are not normally used due to the lack of considerable amounts of quality products [11]. In these locations, it is even more important, to perform new assessments to ensure that the system performs adequately, since, due to the outdoor climate, building use and cultural habits, the system can be subjected to different loads and behave inadequately.

It must be ensured that this system can withstand the demanding Nordic climates, especially in Winter [13], but also due to the fact that it is known that timber-based systems [14–16] and highly insulated systems [17] are prone to mould when combined with insufficient ventilation. Mould usually appears due to the unwanted storage of moisture within the assembly caused by one or more than one possible reasons [17], although specific conditions have to be maintained for certain periods of time for it to grow [18,19]. The existence of mould will eventually lead to loss of integrity, functionality and durability of timber constructions [17], as well as being a risk concerning the health of the building's occupants [20].

In some European countries, the design of an assembly, i.e. choosing its layers and respective thickness, is normally carried out solely concerned with the thermal behaviour of the building, i.e. leaving out its hygric behaviour, which is a key parameter for the longevity of the building [14]. In other countries, like Norway, both behaviours are considered in the design phase of the assembly. This, evidentially, means that the building will be able to withstand current climate, since the design is normally performed assisted by one-dimensional commercial software that already uses built outdoor climate files [19]. In addition, the use of this type of software has the great advantage of allowing a rapid test of the proposed assemblies before application whilst considering different climates, which include precipitation and radiation, user behaviour and initial conditions [21]. This type of software can be used in proficient probabilistic-based methodologies or parametric studies that aim to reduce the risk of facade deterioration [17,22–24] and that can even be used to design a facade that is fitted for specific parameters, e.g. outdoor climate.

This approach has great advantages, but also some drawbacks. One of the main concerns with this approach is that since the buildings are yet constructed, the carried-out simulations use standard based indoor conditions (e.g. [11,25]), which may not reflect reality accurately. In addition, the use of built-in weather files can be outdated or not represent the climate for the case-study location adequately. Even using a one-dimensional (1D) software, important phenomena that can jeopardize the performance of the assembly, can be left out, such as, the air infiltration due to weak points that can be left out due to the 1D sections approach.

This paper aims to develop a multi-step methodology that allows the design and assessment of hybrid facade systems that can withstand current real conditions without being prone to mould. This methodology was developed for a hybrid timber and aluminium unitized facade system for new buildings in order to assess their performance prior to their construction, but it can also be applied to existing buildings or other types of facade systems that will be subjected, for example, to rehabilitation. In addition, by using commercial software, other authors can replicate this methodology. Consequently, it will also be shown the key importance of building current climate files based on long measured datasets, as well as the impact of initial moisture content on the long-term performance of the facade system, which simulated unproper transport and storage conditions of the facade units. Finally, the energy performance of the HUF facade for different Norwegian climates will also be discussed, as well as the importance of the hygric properties of the surface wood treatment on the drying capacity of the HUF facade.

The facade system will be assessed by means of developing computational models, both at the assembly level (using the software WUFI®Pro [26]), as well as at the building level (using the software WUFI®Plus [27]). The first level model will allow to perform thorough hygrothermal analysis of the facade system in terms of mould growth using WUFI Bio [28]. The second level model will be used to obtain the indoor conditions – i.e. temperature and relative humidity – that the first level model needs as an input to run (similar to what was done in Ref. [29]). This latter option has the advantage of obtaining the indoor conditions while taking into account a great number of parameters that affect the indoor conditions that are typical to a building (e.g. geometry, assemblies, internal loads, etc. [30]).

Due to today's availability of weather files in software, like Meteonorm [31], or in online databases, like the CBE Clima Tool [32], it is very straightforward to run simulations for the available locations to test a specific facade system or a rehabilitation measure for a building. However, this option also has its drawbacks, more precisely when one is calibrating models, it is of key importance to use data from the vicinity of the case-study, as well as data that has been recorded during the monitoring campaign as shown by Coelho et al. [33], or even when it is necessary to simulate a specific location, and the nearest weather file corresponds to a location that is several kilometres away and, therefore, the meteorological parameters in the weather file are not representative of the case-study location.

In addition, it is also necessary to account for the following facts: 1) the meteorological data used to build these weather files can be old and, therefore, not representative of today's climate anymore, which means that the carried out simulations are not valid for current conditions; 2) the methodologies used to obtain the meteorological data under the conditions that the software needs are normally not mentioned, which means that the user does not know how the data was obtained; 3) the missing data can be interpolated from nearby weather stations or obtained from satellite data, and, therefore, the weather file is not based on measured data; and 4) the weather files can be based on time periods higher or shorten than what is necessary or recommended. For example, Meteonorm weather files correspond to 10-year periods, while World Meteorological Organization (WMO) states that weather files should be based the closest as possible to a 30-year period [34].

Finally, the choice in terms of type of weather file is, of course, dependent on the goals of the project [35]. For instance, for hygrothermal simulation it is of key importance to account for precipitation [36], and therefore, it is advisable either to use a *test reference year* [37] or a *moisture design reference year* [38], while for thermal simulations precipitation is not necessarily considered [39]. These pointed out aspects lead to the notion that in order to carry out accurate and complete simulations, a great flexibility is needed, which is obtained by means of developing your own weather files fitted for the project goals, which are based on current monitored data for long periods of time, i.e. approximately 30-years of monitored data [34].

In order to make this study more comprehensive and, at the same time, determine how differently the facade system will perform under different climates, three Norwegian climates will be used in the simulations – i.e. Oslo, Trondheim and Tromsø. Norway has a variable outdoor climate depending on the location with the country being divided in temperate climate, continental climate and arctic climate [13]. The option of simulating three different climates will allow to determine the effects of the outdoor climate and, if necessary, make the appropriate changes to the facade system, depending on the location and outdoor climate (e.g. [40]).

These outdoor weather files were built using multi-year data recorded by weather stations that are included in the Norwegian Centre for Climate Services [41] and following the procedure described in ISO 15927–4 [37]. However, due to several reasons, the used datasets have gaps, which had to be artificially filled, just like *Geving and Torgersen* [42] have done when they built the representative weather files for

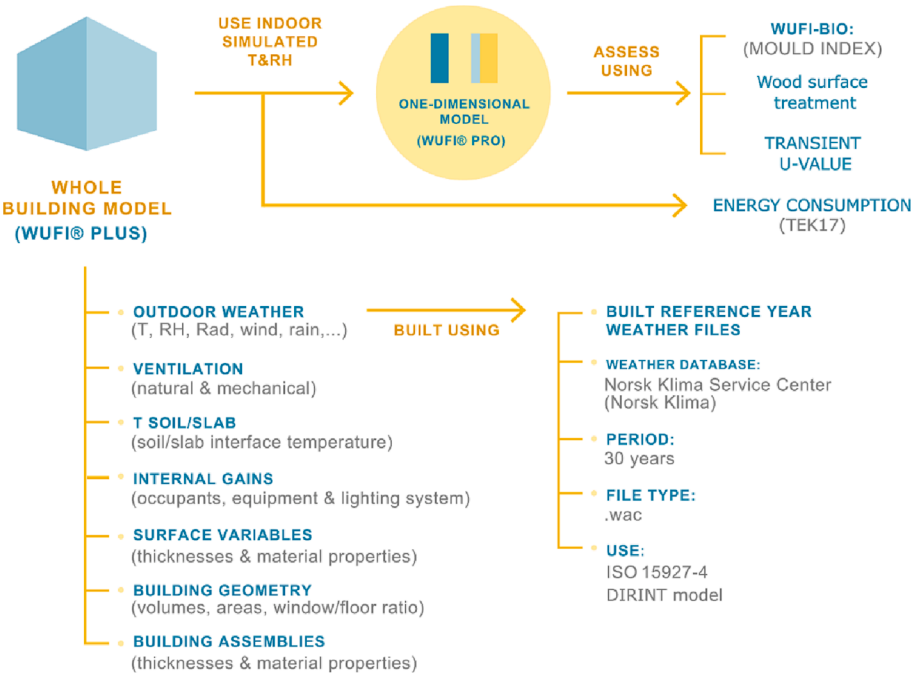

Fig. 1. Overview of the described study methodology.

Norway in 1997 based on measurements that range between 1965 and 1994. The process of finding and filling the gaps was performed by a code developed for that purpose due to the enormous size of the datasets and also to make this process time efficient and less prone to human error [30].

Finally, as pointed out by Pastori et al. [4], a great number of studies of hybrid facade system that analyse their structural behaviour can be found in literature, whereas studies that analyse the hygrothermal behaviour of these type of systems are scarce. Hence, one of the goals of this study is to increase knowledge about their hygrothermal behaviour.

2. Methodology

In order to assess the risk of mould growth in the facade system, a four-step procedure was developed (Fig. 1), which includes the following: 1) develop the *whole-building model* using WUFI®Plus [27]; 2) develop the *test reference year* weather file using ISO 15927–4 [37]; 3) develop *one-dimensional models* using WUFI®Pro [26]; 4) assess the *risk of mould growth* using WUFI Bio [28]. The whole-building model (step #1) will be run for three locations – Oslo, Trondheim and Tromsø – to determine their respective indoor conditions – i.e. temperature and relative humidity. These values will be then used as inputs for WUFI®Pro so that the interior conditions across the facade are obtained. These outputs will be used in WUFI Bio to assess the risk of mould growth and to assess the transient U-value of the selected sections. Energy consumption will be compared to TEK17 limits [43].

In order to make this process time-efficient, the interconnections between the methodology steps were performed using MATLAB. For instance, the indoor relative humidity was calculated, for each location, following the procedure described in standard EN 13788 [44] for the attached zones. The indoor conditions – temperature and relative humidity – obtained from WUFI®Plus for the 7th floor were transformed into a .WAC file for WUFI®Pro [45]. Lastly, the transient U-value is also calculated using MATLAB, as well as assessing the energy consumption [46].

The outdoor weather files were built using about 30-years' worth of data – January 1990 until December 2019 – downloaded from the website of the Norwegian Centre for Climate Services [41] and based on the methodology described in ISO 15927–4 [37]. It is normal that for monitored data that there are gaps within its records due to one of many reasons [47]. To fill these gaps, one of two methodologies were applied, which depended on the gap length [37,48]: 1) *Minor gaps* (i.e. smaller than 3 h) – linear interpolation; and 2) *Major gaps* (i.e. bigger than 3 h) – cubic spline. This procedure was applied to all meteorological data used to build the outdoor weather files (Fig. A1), which saved a lot of data processing time.

2.1. Computational models

2.1.1. WUFI pro

The StaticusCare project [3], which is financed by EEA/Norway Grants, aims to develop a hybrid timber and aluminium facade systems that seeks to reduce the CO_2 footprint of the facade system between 70 and 75% and the non-renewable energy consumption between 53 and 56%. This CO_2 footprint reduction is expected to occur due to the partial replacement of the aluminium by timber, since the traditional frames of this type of facades are in aluminium, and the preparation for usage in buildings is a much more polluting process than the one that timber has to go through in order to be applicable in buildings [5]. The non-renewable energy consumption is expected to decrease because timber is also a much more thermal efficient material than aluminium [5].

Nonetheless, it is extremely important to guarantee the quality of this new facade system, especially in such demanding outdoor conditions, as those existing in Nordic countries. For this purpose, a complex hygrothermal software tool (WUFI®Pro) is used to thoroughly assess the performance of this system. The WUFI®Pro models need the following main inputs to run to their fullest capacity [49]: 1) the basic and advance building properties of the materials, which can be selected from WUFI material database; 2) the outdoor weather file, which can be selected from WUFI database or built; and 3) indoor conditions, which can be obtain from a specific standard or set in manually. The developed hygrothermal simulations were carried out considering the heat and moisture balance equations and the thermal dependency of temperature and moisture [50,51].

In this project, this latter type of input will be obtained from WUFI®Plus for a specific case-study (2.1.2). Finally, the hybrid timber and aluminium facade system is constituted by the following layers (Fig. 2):1) Frames – made from glue laminated timber beams (coated)

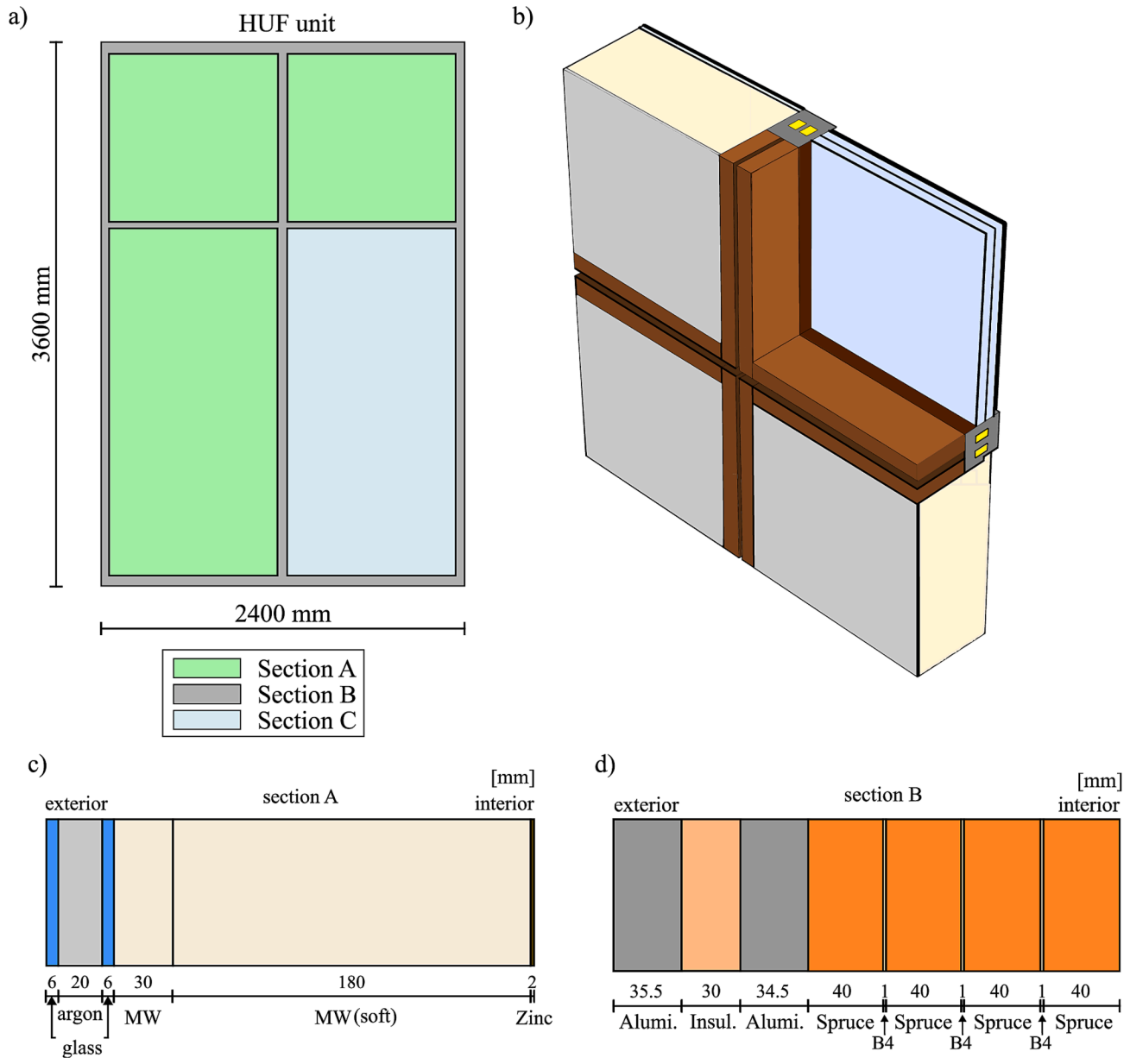

Fig. 2. Hybrid unitized facade system (a) and a 3D view of an example of a section of the system seen from the interior (b) (based on Ref. [54]), as well as section A (c) and section B (d) of the facade system.

and aluminium profile; 2) Opaque zone – bended tin sheet, mineral wool insulation, external finishing: Powder coated external aluminium tin sheet and enamelled glass; and 3) Transparent zone – triple glazed glass unit. Section A (Fig. 2c) is composed transversally by enamelled glass, mineral wool and zinc and has a surface area in each Hybrid Unitized Facade (HUF) unit of ca. 5.1 m^2. Secondly, section B (Fig. 2d) is composed transversally by aluminium and spruce and has a surface area in each HUF unit of ca. 1 m^2. Lastly, section C is a triple glazed glass unit with a $U_{w\text{-}value}$ of 0.5 W/m^2K.

Most of the material properties used in this project are from WUFI database [27], but some of these properties were changed in accordance with the real materials used in the facade system. Some properties were also taken from EN ISO 10456 [52] when the WUFI database did not have the necessary material (e.g. zinc). An overview of the materials' most important hygrothermal properties, which were used in both type of models, is presented in Table 1. A wood surface treatment with a S_d-value of 0.5 m, which is assumed as the limit for an "open" diffusion treatment [53], was included in the interior surface of section B.

The outdoor weather files for Oslo, Trondheim and Tromsø, which were developed using the methodology described in subsection 2.2, were used for the developed models. The one-dimensional model allows to select the position(s) that the user sees fit to assess [26]. Hence, specific locations were selected and assessed in terms of mould growth risk using WUFI Bio [28] (see Fig. 6d and e). The *U-value* of the assessed sections was calculated in accordance with the variance of the moisture content in the hygroscopic materials and the variance of the exterior heat resistance that varies in accordance with the wind conditions (as described in 2.4.2). In addition, to the wind-dependent exterior heat resistance, and consequently, the exterior water vapour transfer coefficient, the 0.125 (m^2K)/W was adopted for the interior heat resistance. The default 0.7 adhering fraction of rain was adopted, but the short-wave radiation absorptivity changed in accordance with the tested section, 0.05 for section A and 0.14 for section B.

2.1.2. *WUFI plus*

The case-study is an eight-floor office building with a floor area of

Table 1
Hygrothermal building properties of the materials used in the developed models (data taken from WUFI material database [27] and EN ISO 10456 [52]), respective layer thickness, thermal resistance and thermal transmittance. The material correspondent thermal resistance is also shown in terms of percentage of the assembly's thermal resistance.

Sect	Code	Material	Thick. d, m	Hygrothermal properties					Thermal resistance		U-value
				Bulk density	Porosity	Heat capacity	Thermal conduct.	Vapour diff. resist. factor			
				ρ, kg/m^3	ε, m^3/m^3	c_p, J/(kg.K)	λ, W/(m.K)	μ, [-]	(m^{2}K)/W	%	W/(m^{2}K)
A	A1	**Glass** (2 layers)	0.006	2,500 [52]	0.001 [27]	750 [52]	1.000 [52]	50,000 [27]	0.01	0.2	0.129
	A2	**Argon**	0.020	1.7 [52]	0.999 [27]	519 [52]	0.017 [52]	1 [52]	1.18	15.5	
	A3	**Minewool** (semihard)	0.030	40.0 [27]	0.950 [27]	1,030 [27]	0.031 [27]	1 [27]	0.97	12.7	
	A4	**Minewool** (soft)	0.180	25.2 [27]	0.950 [27]	1,000 [27]	0.033 [27]	1 [27]	5.45	71.7	
	A5	**Zinc**	0.002	7,200 [52]	0.001 [27]	380 [52]	110 [52]	50,000 [27]	0.00	0.0	
	Total		0.244	–	–	–	–	–	7.61	–	
B	B1	**Aluminium**	0.070	2,700 [27]	0.001 [27]	900 [27]	200 [27]	50,000 [27]	0.00	0.0	0.375
	B2	**Polyisocyanurate insulation**	0.030	32.5 [27]	0.999 [27]	1,470 [27]	0.024 [27]	72 [27]	1.25	50.1	
	B3	**Spruce** (4 layers)	0.040	390 [27]	0.750 [27]	1,600 [27]	0.13 [27]	108 [27]	1.23	49.4	
	B4	**Glue** (3 layers)	0.001	1,200 [52]	0.001 [52]	1,800 [52]	0.25 [52]	6,000 [52]	0.01	0.5	
	Total		0.263	–	–	–	–	–	2.49	–	

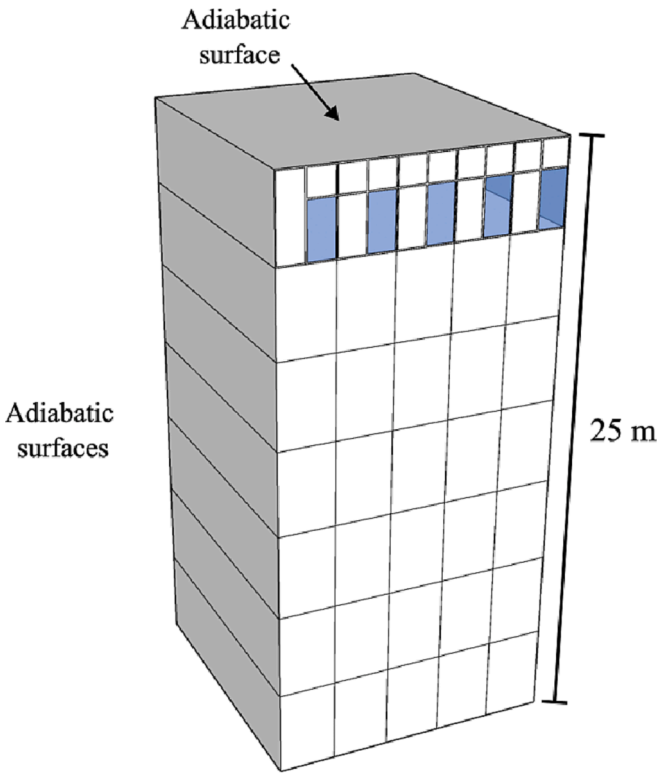

Fig. 3. SketchUp render of the simulated case-study.

150 m^2. The only simulated floor was the 7th floor, whilst the other floors were assigned as attached zones (conditioned spaces). This option enable to consider the highest driving rain load on the facade system using the WUFI method [26] without having a much longer computation time [33]. The simulated floor is equipped with a mechanical device that heats and cools the indoor climate in accordance with the setpoint strategy and another device to ensure a proper ventilation.

One side has the facade system (i.e. side shown in Fig. 3), which corresponds to the orientation with the highest wind-driven rain (WDR). For Oslo, this orientation corresponds to *South*, but for Trondheim it corresponds to *Southwest* and for Tromsø it corresponds to *West*. Note that these orientations were used for both the WUFI®Plus as well as the WUFI®Pro simulations. The other sides are considered adiabatic, so that this case-study can be representative of a larger building, i.e. a multi-floor building.

The internal gains, ventilation rates and setpoint strategy used in this model are in accordance with the values recommended for office buildings by SN-NSPEK 3031:2021 [55], which will be explained in subsection 2.3. The same assemblies as described in subsection 2.1.1, i.e. in terms of layers hygrothermal properties and respective thicknesses, were used for the WUFI®Plus model with the addition of the transparent zone, which is a triple glazed glass unit. The outdoor weather files that were used, were built using the methodology described in 2.2.

The computational model was run for each of the selected conditions thus obtaining their respective indoor conditions – temperature and relative humidity. These conditions were then used as input for the one-dimensional model of the system, which allows a more thorough assessment of the hygrothermal behaviour of the facade system. The geometry of a generic office building was developed in SketchUp (Fig. 3) and then transferred to WUFI Plus using the SketchUp plug-in [27]. This is an interesting tool because it allows to build complex geometries more easily. Alternatively, one can also use the gbXML importer which enables to import Revit models [33], which is an interesting tool for new projects, due to today's extensive use of tools like Revit.

2.2. Outdoor weather files

Due to Norway's different climate types (Fig. 4), the following study included three locations: 1) Oslo (lat. 59.94 N and long. 10.72° E), 2) Trondheim (lat. 63.41° N and long. 10.45° E) and 3) Tromsø (lat. 69.65° N and long. 18.91° E). Due to Norway's comprehensive meteorological system [41], each of these locations has several stations. However, not all stations have the necessary data for WUFI simulations [56] or for all the necessary period (ca 30 years [57]). Hence, a thorough data assessment was carried out in the *Norwegian Centre For Climate Services*

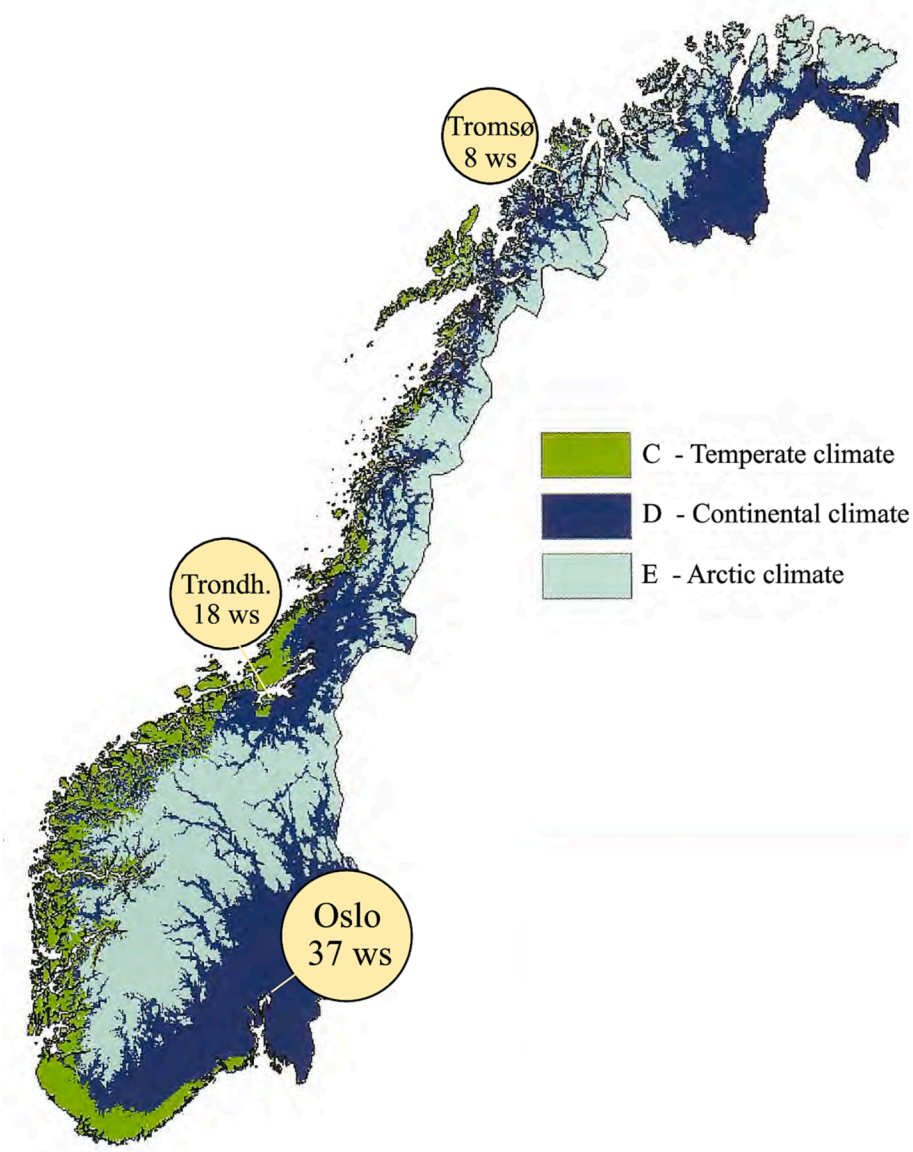

Fig. 4. Köppen climate classification of Norway and respective assessed weather stations (ws) for each of the three selected locations (map adapted with permission from Ref. [13], SINTEF Byggforsk 2007).

Table 2
Main selected meteorological stations for each location – Oslo, Trondheim and Tromsø.

Nr	Location	Selected Meteo. Station					
		Name	Code	Height above MSL	Lat.	Long.	Operating period
1	Oslo	Blindern	SN18700	94 *m*	59.94° N	10.72° E	01.01.1931 – now
2	Trondheim	Voll	SN68860	127 *m*	63.41° N	10.45° E	01.01.1923 – now
3	Tromsø	Tromsø (Holt)	SN90400	20 *m*	69.65° N	18.91° E	04.05.1987 – now

online weather database [41] for each of these locations and the most data complete station was selected for each of the locations (Table 2). A total of 63 meteorological stations were assessed for these three locations (Fig. 4).

For WUFI to run to its fullest capacity, the following meteorological conditions, preferably in hourly values, are necessary [27]: 1) temperature, 2) relative humidity, 3) air pressure, 4) global radiation, 5) diffuse radiation, 6) atmospheric counter radiation, 7) precipitation, 8) cloud index, 9 & 10) wind direction and speed. However, there are some parameters that can be considered more fundamental than others. A mean value for the *air pressure* can be assumed, due to its small effect on the results [27]. In addition, the *atmospheric counter radiation* and *cloud index* should only be considered if radiation cooling is going to be studied [27,58].

Hence, the initial station assessment for the time period that is defined between January 1990 and December 2019 – i.e. a 30-year period – is limited to 5 variables [41], namely: temperature (T), relative humidity (RH), global radiation (GR), precipitation (P), and wind direction (WD). Normally, a combined apparatus is used to measure both the wind direction and speed [47], hence if the station has values for one, it has for the other. At a later stage, the air pressure at the station location (AP) and wind speed (WS) were also checked for each location.

Table 3
Assessment of the meteorological data for *Oslo* (Blindern station), *Trondheim* (Voll station) and *Tromsø* (Tromsø (holt) station) and respective recorded data in each period, in percentage (<50 % is red, 50–90 % is yellow and greater than 90 % is green).

Station	Batch	Periods	Precip.	Temp.	Wind direction	Global radiation	Relative humidity	Air pressure	Wind speed
Blindern (SN18700)	1	01/12/1992 31/12/1999	67%	97%	97%	45%	97%	97%	97%
	2	01/01/2000 31/12/2009	30%	100%	100%	63%	100%	100%	100%
	3	01/01/2010 31/12/2019	94%	100%	100%	50%	100%	100%	100%
Voll (SN 68860)	1	01/09/1996 31/12/1999	97%	97%	97%	69%	97%	97%	97%
	2	01/01/2000 31/12/2009	66%	100%	100%	100%	100%	100%	100%
	3	01/01/2010 31/12/2019	82%	99%	99%	12%	99%	99%	99%
Tromsø (SN 90400)	1	29/07/1998 31/12/1999	99%	99%	0%	98%	99%	0%	0%
	2	01/01/2000 31/12/2009	100%	100%	0%	96%	100%	0%	0%
	3	01/01/2010 31/12/2019	99%	100%	0%	80%	100%	0%	0%

For some of the selected locations, weather data was missing in short/mid periods of time, or it did not even exist for the analysed period (Table 3). For these purposes, the missing weather data was obtained using other tools (e.g. *solrad.xls* [59], which is based on the model described in Ref. [60], when the global radiation data was missing) or even using the data from the nearest stations.

The selected 30-year period was divided in three 10-year periods to ease the analysis process. The starting point for the first 10-year period changes in accordance with the starting date in which the data started to be measured hourly. This means that the number of years used to build each weather file varied, but all were above a 20-year period – i.e. 27 years for Oslo, 23 years for Trondheim and 21 years for Tromsø. This means that the weather files are based on the following dataset sizes: ca. 236 K measured data points per meteorological variable for Oslo, i.e. 1.6 M in total; ca. 201 K measured data points per meteorological variable for Trondheim, i.e. 1.4 M in total; and ca. 183 K measured data points per meteorological variable for Tromsø, i.e. 1.2 M in total. The following options were taken to have a nearer complete set of data (i.e. above the 90 %-limit in Table 3):

Oslo – Blindern station: Precipitation will be filled by values from *Blindern Plu station* (SN18701) and the measured global radiation values for Blindern station will be artificially filled using the *solrad.xls*;

Trondheim – Voll station: Precipitation will be filled by values from *Kvithamar station* (SN69150), and the global radiation will be filled using the *solrad.xls*;

Tromsø – Tromsø (holt) station: Both the wind direction and wind speed will be filled by values from the *Hekkingen Fyr station* (SN88690), whilst the air pressure will be filled by values from *Torsåg Fyr station* (SN90800). Finally, the global radiation will be filled using the *solrad.xls*.

The *test reference year* weather files were built using the methodology described in ISO 15927–4 [37], which builds a representative year based on multi-year hourly data of, at least, four meteorological variables, i.e. temperature (°C), relative humidity (%), global radiation (W/m^2) and wind speed at 10 m above ground (m/s). Note that the final selected month is also applied to the remaining meteorological variables that WUFI needs in order to run hygrothermal simulations. Secondly, the *Perez model* (DIRINT) was used to divide the global radiation in its direct and diffuse components [61,62], since WUFI software needs both the global and the diffuse radiation to run [26,27]. All operations related to the building of the weather files were performed using MATLAB, so that the process is time-efficient and less prone to error [30].

The DIRINT model corrects the DISC model [63] through a coefficient that is obtained from a four dimensional look-up table that is based on the bins presented in table 1 of Ref. [61]. The following parameters are used to obtain this coefficient for each timestep [61]: 1) solar zenith angle, 2) clearness index, 3) atmospheric precipitable water, and 4) stability index. Air temperature and relative humidity are necessary to determine the precipitable water [64].

The DISC model [63] needs extraterrestrial radiation, which is determined using Spencer's equation [65], to determine the direct radiation. The solar zenith angle is determined using the MATLAB code developed by Mikofski [66], which was tested by Coelho [67] for Lisbon and it obtained low error when compared with another reliable solar position calculator [68]. The air mass, which is needed for the DISC model [63], is calculated using the Kasten equation with the revised constants [69] and adapted for the local conditions [65] with the pressure at the weather station varying with time. The dew point temperature was obtained using equation in Ref. [70], which needs air temperature (°C) and relative humidity (-). The global radiation irradiance is then related with the direct normal irradiance and diffuse horizontal irradiance [71].

Lastly, to validate the code, the results of each section of the code were compared to results obtained from reliable tools. The *direct normal irradiance* obtained from the DISC model ($I_{b,disc}$) values for Oslo (59.94° N and 10.72° E) were compared to the values obtained from the excel DISC model [72]. The *direct normal irradiance* obtained from the DIRINT model (I_b) values were compared against the results obtained from *pvlib. irradiance* [73] for data taken from Florida Uib station in the Bergen region for 2022. This is the only station in Norway that currently measures both the global and diffuse radiation and it has more than one year of radiation data available [41]. The yearly differences between the measured and simulated diffuse radiation was 12.6 %, which fits within the error margins that Meteonorm presents in its validation procedure [74], which validates the developed MATLAB code.

Finally, the weather files were produced in .WAC type, which is a flexible type of climate weather files [26]. Table 4 presents an initial assessment in terms of temperature, relative humidity, precipitation and radiation for each of the selected climates for the weather files built for this study, as well as for the weather files built by *Geving and Torgersen*

Table 4
Overview of the outdoor climates for the three selected locations built for this study (named, OsloMet) and built by Geving and Torgersen [42] (named, NTNU).

Locat.	Source	Temperature (°C)			Relative humidity (%)			Normal rain (mm/a)	Avg. global Rad. (W/m^2)	Heating Degree-days (°C)	Heating season (days)
		Min	Mean	Max	Min	Mean	Max				
Oslo (orient: **S**)	OsloMet	−15.0	7.4	31.5	19	76	100	1037	151.25	4031 ± 124	221 ± 10
	NTNU	−14.8	6.8	29.3	15	73	100	605	–	–	–
Trondheim (orient: **SW**)	OsloMet	−12.8	6.1	26.5	25	77	100	1167	139.47	4053 ± 87	250 ± 12
	NTNU	−13.8	5.4	24.2	46	88	100	1234	–	–	–
Tromsø (orient: **W**)	OsloMet	−11.7	4.1	24.0	25	79	100	828	122.01	4802 ± 34	293 ± 13
	NTNU	−14.2	2.1	22.0	29	82	100	1276	–	–	–

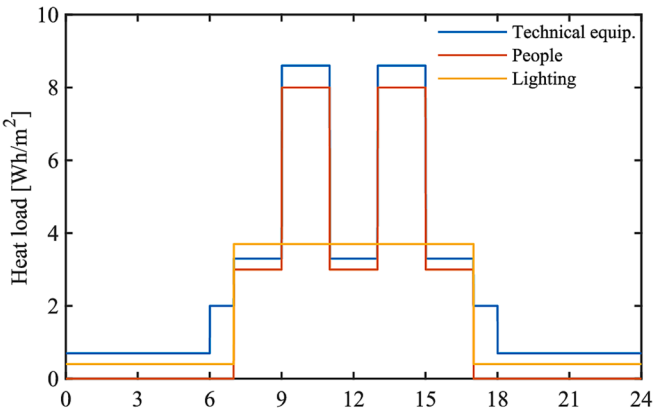

Fig. 5. Internal gains profile for office buildings – for technical equipment, people and lighting system – in accordance with SN-NSPEK 3031 [55].

[42], which used monitored data from 1965 to 1994 (30 years) in half of the twelve selected locations. The length of the datasets used to build the weather files were the following [42]: 20 years (1975 to 1994) for Oslo, 17 years (1965 to 1981) for Trondheim and 30 years (1965 to 1994) for Tromsø, with data being normally taken three times a day – 7:00, 13:00 and 19:00, but some stations also recorded measurements at 1:00.

It is visible that there has been a general increase of temperature in the three locations, which is reflected as a lower minimum temperature and a higher average and maximum temperatures (Table 4), which is in line with the DNMI report 01/02 [75]. These behaviours are more substantial for Tromsø, where the annual average increased 2 °C. On the other hand, the relative humidity decreases in terms of annual average and minimum temperature for Trondheim and Tromsø, but there is an opposite behaviour for Oslo. Finally, the precipitation has a substantial increase for Oslo (i.e. 432 mm) and a substantial decrease for Tromsø (i.e. −488 mm). In Trondheim, the precipitation has a slight decrease of 5.4 %. A comparison between the values from the two weather files origin – OsloMet & NTNU – was performed. Although this is an interesting initial assessment, it is important to consider that the methodology followed to build the weather files is different and that the data has different frequencies, which in turn influences the results.

The heating degree days (HDD) and the heating season were determined using the methodologies described in Ref. [75]. For the studied period, i.e. ca 30 years, the heating season in Oslo decreases with a rate of 0.5 days per year, and the heating degree days also decrease at a rate of 1 °C per year. The same behaviours are observed for Trondheim, in which the heating season decreases with a rate of 0.25 days per year, and the heating degree days decrease at a rate of ca 1 °C per year. Finally, in Tromsø the heating season decreases with a rate of 0.15 days per year, but the heating degree days increase at a rate of ca 0.32 °C per year. Most of these occurrences were caused by the increase of global air temperature that occurred worldwide during the studied periods [76].

2.3. Internal gains, ventilation rates and setpoint strategy

The internal gains, ventilation rates and setpoint strategy used in this study are in accordance with the values recommended for office buildings by SN-NSPEK 3031:2021 [55]. Fig. 5 presents the day-profile for the heat load that has to be considered for office buildings according to this Norwegian specification [55]. This day profile accounts for the contribution of the lighting system, people and technical equipment. The assumed ventilation rates was 7 $m^3/(h.m^2)$ during operating hours and 2 $m^3/(h.m^2)$ outside operating hours [55], which means 1050 m^3/h and 300 m^3/h for a floor area of 150 m^2. Lastly, the followed temperature setpoint strategy was 21 °C for minimum and 24 °C for maximum temperature in accordance with the recommendations set by SN-NSPEK 3031:2021 [55]. For this work, a metabolic rate of 1.2 met was assumed, which corresponds to sedentary activities performed in offices [77].

WUFI®Plus needs the internal gains separated in the following four parameters: 1) heat production, which is subdivided in heat convective and heat radiant, both in W; 2) moisture production in g/h; 3) CO_2 production in g/h; and 4) human activity in met [27]. Hence, some conversions had to be performed to make the SN-NSPEK 3031 internal gains profile in accordance with the requirements set by WUFI®Plus. A similar methodology as described in Ref. [33] was applied.

The polynomial function, used by EnergyPlus [78], was applied here to divide the total heat generated by the building's occupants in its sensible heat and latent heat parts. The sensible heat load was divided in its radiant and convective parts in accordance with the recommendations set by ASHRAE Fundamental Handbook [79] for office buildings, i.e. 60 % for radiant heat and 40 % for convective heat. An indoor average temperature of 21 °C was assumed in accordance with recommendations set by SN-NSPEK 3031:2021 [55]. For the other internal gains, a 0.5/0.5 split was used for the technical equipment and a 0.58/0.42 split was used for lighting, as advised by Ref. [79].

In WUFI®Plus, the latent heat load is treated as moisture, which is obtained by dividing it by the water enthalpy of evaporation, which decreases with temperature [8,80]. In this study, a value of 2452 kJ/kg was assumed. Finally, the CO_2 generated by the building's occupants was determined using the equation presented in standard ASTM 6245 [81]. This rate has to be multiplied by the CO_2 density in gaseous state, i.e. 1883 g/m^3 at 21 °C and 1 atm [82], so that the values appear in g/h.

2.4. Performance assessment tools

2.4.1. WUFI Bio

In timber-based constructions, one of the most worrisome problems is the grow of mould. This is mostly due to its degradation power and due to health concerns [83]. These problems can be prevented if a proper facade design is preformed, more even if dynamic calculations are carried out using, e.g., advance software like WUFI Pro and Bio.

These tools allow to test, for a given location (i.e. a certain weather file), if there is risk of mould growth, and, if this risk is serious, to make the proper modifications to the designed facade. Of course, for mould to grow, a specific relative humidity has to be achieved, which will depend on the temperature and the specific nature of mould, the duration of exposure, but it is also necessary that the substrate has nutrients [18].

In this study, the mould growth was assessed using the *mould index* [84,85], which is time dependent, and it can be classified between 0 and 6, which respectively corresponds to a "clean surface" and a "surface that has been totally cover by mould" [28]. The safety-limit is 2.0 for "surfaces inside constructions without direct contact with the indoor climate" [28] and it is 1.0 for "indoor surfaces in contact with the indoor climate" [28] to prevent damage from mould and health problems for the occupants.

The original VTT/Viitanen model, which is an empirical model based on visual findings of mould growth, was created by laboratory experiments run for sapwood with constant conditions [86]. Subsequently, the model was updated based on the studies developed by Hukka and Viitanen [85] in 1999 in which they considered varied and variable humidity conditions. More recently, a relationship was developed between the VTT model and the biohygrothermal IBP model [18] through a transfer function based on a large and varied number of simulations run in WUFI Pro that transforms the calculated growth (in mm) into the mould index [84]. This is the basis for the Mould index values that are obtained in WUFI Bio used in this study.

To ease the assessment of the mould index results, a new concept of *total mould index sum* was introduced, which is defined as the sum of the mould indexes that are above the safety limit for the select period being time and occupant exposition class dependent, namely:

$$MI_{sum} = \sum_{i=1}^{n} (MI_i - MI_{SL}) when MI_i > MI_{SL} \quad (1)$$

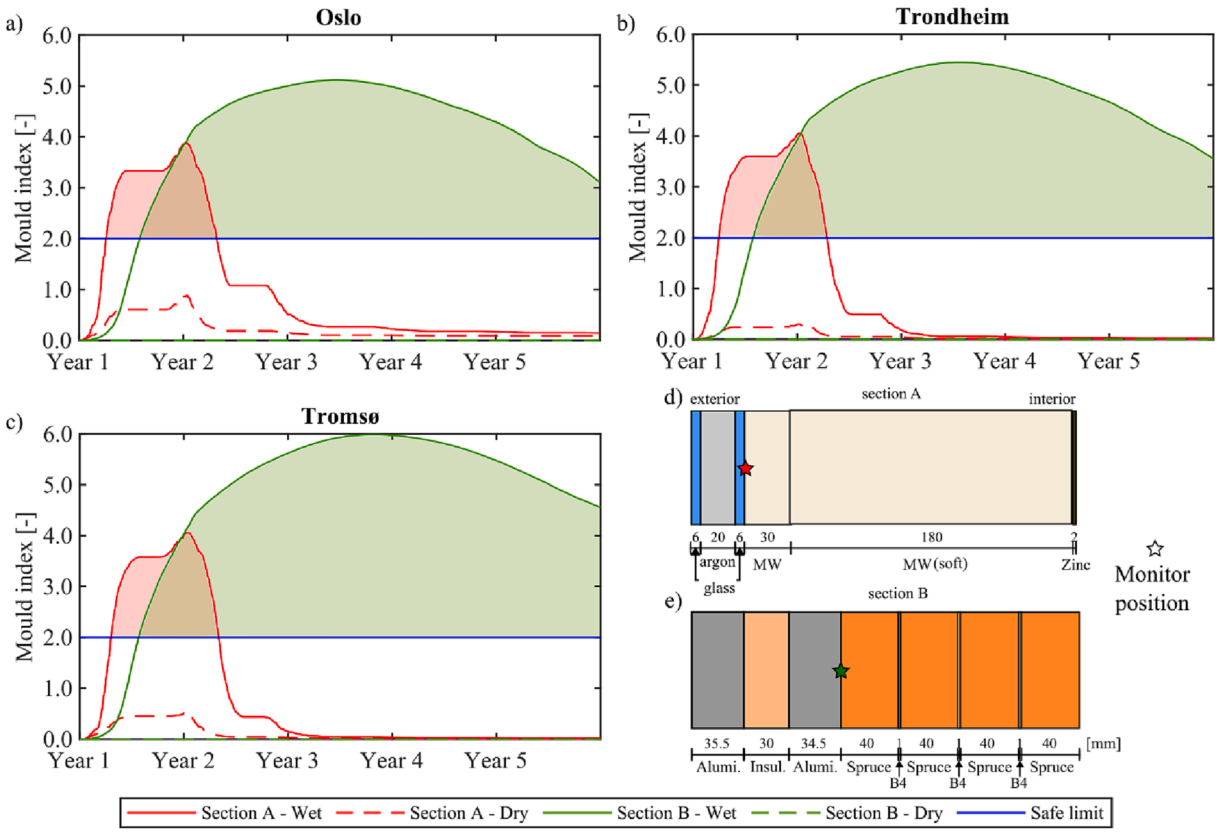

Fig. 6. Mould index for the five simulated years for Oslo (a), Trondheim (b) and Tromsø (c) for section A (d) and section B (e) with dry conditions (i.e. 60 %RH initial) and wet conditions (i.e. 80 %RH initial).

where MI_{sum} is the total mould index sum (-), MI_i is the mould index for instant i above the safety-limit (-), MI_{SL} is the mould index safety limit (-), which is dependent on the occupant exposition class [28].|

2.4.2. *U-value moisture-dependent*

The *U-value* (W/m^{2}K), or thermal transmittance, is a parameter that allows to quickly and easily compare different buildings assemblies, i.e. walls, ceilings, roofs, floors, in terms of energy efficiency performance [87]. A higher value means that the amount of energy that is transmitted through the assembly, per area and temperature difference, is higher, whilst a lower U-value means the opposite [87]. However, due to the capacity to store moisture in the large majority of the materials used in building construction [88], this U-value can vary significantly throughout the year in accordance with the assembly composition and outdoor conditions [36]. This moisture dependency of hygroscopic materials is taken into account by calculating a thermal conductivity that increases with the amount of moisture [89], by means of the following equation:

$$\lambda_m = \left(\lambda_0 + b \bullet \frac{w}{\rho_s}\right) \tag{2}$$

where λ_m is the moisture dependent thermal conductivity (W/(m.K)), λ_0 is the thermal conductivity at dry state (W/(m.K)), b is the thermal conductivity increase induced by moisture amount (%/M.-%), w is the moisture content in the building material (kg/m^3) and ρ_s is the bulk density of building material in dry state (kg/m^3).

The *U-value* moisture-dependent can be calculated by means of equation (3) using the building layers properties – i.e. thermal conductivity and bulk density – and respective thicknesses and the moisture content in each building material, which is obtained from WUFI [36]. This alternative procedure allows a great flexibility in terms of data assessment when compared to WUFI postprocessor [26], and it has been used elsewhere (e.g. [25,90]).

$$U_m = \frac{1}{R_{se} + \sum_{t=1}^{t=i} \frac{e}{\left(\lambda_0 + b \bullet \frac{w_t}{\rho_s}\right)} + R_{si}} \tag{3}$$

where U_m is the moisture dependent thermal transmittance (W/(m^{2}K)), R_{se} and R_{si} are the exterior and interior surface heat resistance ((m^{2}K)/W), λ_0 is the thermal conductivity at dry state (W/(m.K)), b is the thermal conductivity increase induced by moisture amount that is material dependent (%/(M.-%)), w_t is the moisture content in the building material at instant t which is obtained from the WUFI simulations in accordance with the chosen inputs (kg/m^3) and ρ_s is the bulk density of building material in dry state (kg/m^3). R_{se} can be calculated in accordance with the wind conditions [26].

3. Analysis and discussion

3.1. *Mould growth assessment*

The most probable risk point was assessed in terms of mould growth for each of the two simulated sections of the HUF unit: 1) in between the glass and mineral wool for sections A (Fig. 6d), and 2) in between the aluminium and the first spruce lamella for section B (Fig. 6e). It is visible that for normal conditions, i.e. when the materials are properly stored and, consequently, their initial moisture content corresponds to 60 % RH, the risk of mould growth is low for any of the studied climates and for both simulated sections (Fig. 6). For the simulated spruce, the 60 % RH corresponds to a moisture content of 41 kg/m^3. This means that the spruce, which has a bulk density of 390 kg/m^3 (Table 1), has initially ca. 11 % of moisture content.

For section B, the mould index is zero for the five years for the three

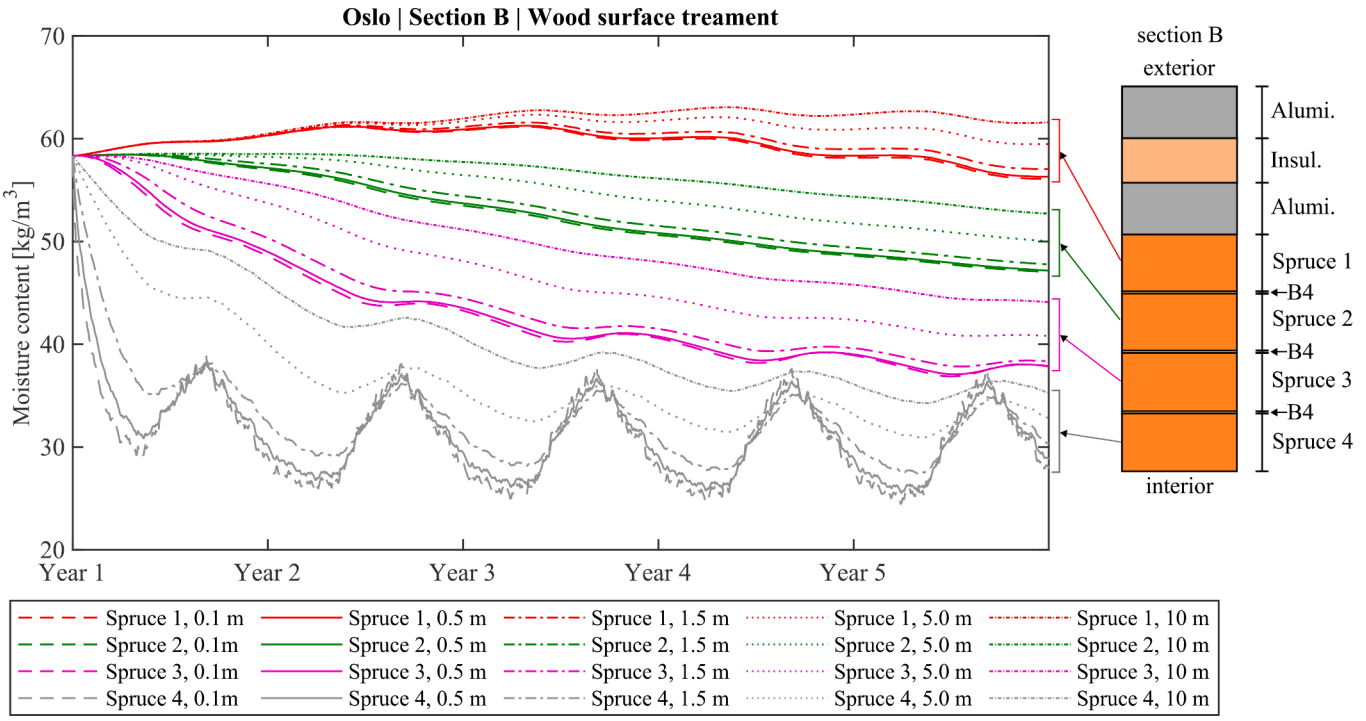

Fig. 7. Moisture content (kg/m^3) for the five simulated years for the four spruce lamellas (spruce 4 is the nearest to indoor surface) for five different wood surface treatment – S_d-value of 0.1 m, 0.5 m (reference), 1.5 m, 5.0 m and 10 m (values taken from Ref. [91]).

simulated climates, but for section A the mould index is higher than zero with Oslo being the climate that attains the highest value – 0.88 (Fig. 6a), while the maximum mould index for Trondheim is 0.30 (Fig. 6b) and 0.54 for Tromsø (Fig. 6c). Nonetheless, the safety limit for the selected conditions is never overcome in any of the tested climates (Fig. 6), which means that the assemblies can prevent moisture that comes from the boundaries, i.e. since the moisture content is decreasing – Fig. 9a for Oslo, Fig. 9b for Trondheim and Fig. 9c for Tromsø.

If the materials are not properly stored, and their initial moisture content correspond to 80 %RH, the moisture tightness of the HUF unit works in its disadvantage, because the assemblies' dry rate is not enough to withstand the higher moisture content level when compared with the normal conditions, and, therefore, the risk of mould growth is much higher (Fig. 6). For the simulated spruce, the 80 %RH corresponds to a moisture content of 58 kg/m^3. This means that the spruce, which has a bulk density of 390 kg/m^3 (Table 1), initially has ca. 15 % of moisture content.

The behaviour of section A is similar for the three locations (Fig. 6), but some minor differences are still detected. In Oslo, the safety limit is overcome for 9,304 h and achieves a maximum value of 3.8, which means that some growth is already detected visually [85], and has a *total mould index sum* of 11,654. In Trondheim, the safety limit is overcome for 9,102 h, which is less than for Oslo, but a higher maximum value of 4.1 is achieved, which means a visual coverage of more than 10 % [85], and has a total mould index sum of 13,058, i.e. 12 % higher than Oslo's. Finally, the safety limit is overcome for 9,054 h in Tromsø, while the maximum value is the same as Trondheim, but the total mould index sum is 13,190, which is slightly higher than Trondheim's, i.e. 1 %.

The differences between the three climates are more pronounced in section B than in section A (Fig. 6). The safety limit is overcome for 38,395 h in Oslo while achieving a maximum value of 5.1, which corresponds to a coverage of more than 50% [85], and the total mould index sum is 92,075. In Trondheim, the safety limit is overcome for 38,747 h, while the maximum value is 5.4 and the total mould index sum is 103,449, i.e. 12 % higher than Oslo's. Finally, the safety limit is overcome for 38,861 h in Tromsø, while the maximum value is 6.0, which corresponds to a tight coverage [85], and the total mould index sum is 124,437, i.e. 20 % higher than Trondheim's. The mould index is eventually able to decrease, because the assemblies are able to dry out (e.g. Fig. 9a–c). In sum, the most worrying case is Tromsø, but closely followed by Trondheim's and Oslo's, if the materials are not properly stored before installation or if there are not safely kept whilst being transported.

3.2. *Wood surface treatment*

The influence of the indoor surface wood treatment in the drying capacity of section B was assessed. In total, five different surface treatments, with different *water vapour diffusion equivalent air layer thickness* (S_d-values), were assessed, namely [91]: 1) *oil emulsion paint* with a S_d-value of 0.1 m, 2) *acrylic paint* with a S_d-value of 0.5 m, 3) *wood preservative* with a S_d-value of 1.5 m, 4) Alkyd paint/varnish with a S_d-value of 5.0 m, and 5) epoxy paint with a S_d-value of 10.0 m. Note that not all of these treatments are usually applied to timber/wood as surface treatments, but the reasoning behind their choice was to test this layer limits using S_d-values from real products.

The surface treatment with a S_d-value of 0.5 m was set as reference because it represents the limit for "open" diffusion surface treatments [53]. It is visible that the surface wood treatment can have a significant influence in the drying capacity of the section, specially the closer the spruce lamella is to the indoor climate (Fig. 7). This is even more noticeable for the first years of the simulations, since there are higher amounts of moisture within the section (Fig. 9). For instance, the maximum difference in terms of moisture content between the wood surface treatment with 0.5 and 10.0 m is ca. 20 kg/m^3 at the beginning of the first year of simulation, but this difference will steadily decrease throughout the years. Even by applying a wood surface treatment with a S_d-value of 0.1 m instead of the 0.5 m differences are visible, more significantly at the beginning of the simulation, since the section will have a higher drying capacity, reaching a lower moisture content by 3.4 kg/m^3 when compared with the reference case.

For the inner lamellas, the difference due to the wood treatment is

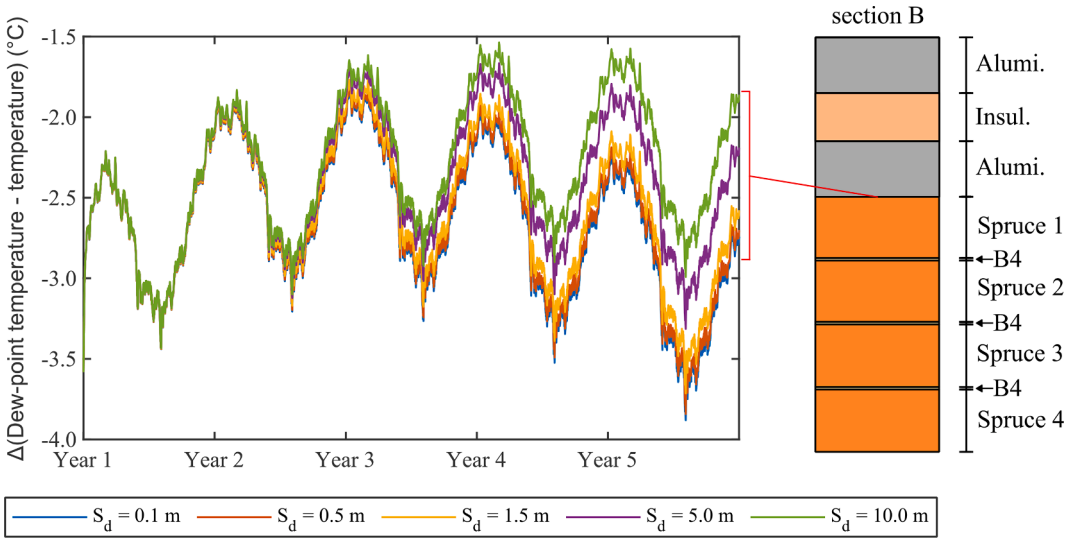

Fig. 8. Difference between dew-point temperature and temperature for the interface between the aluminium and the first spruce for the five tested wood surface treatments and for the five simulated years. Negative values means no interstitial condensation.

only noticeable more down the simulation since they are more limited in terms of drying. For example, for spruce 1, the difference between the applying a wood surface treatment with a Sd-value of 0.5 or 10.0 m is only bigger than 1 kg/m^3 from the end of the second year. However, from then onward this difference will steadily increase throughout the simulated years.

This is normal because the closer the lamella is to the indoor climate, the faster it will dry due to the composition of this section, i.e. using the aluminium in the outer surfaces, the drying will occur and it is govern by the interior side. The inner spruce lamellas (e.g. spruce 1) will also reach these values eventually, but they take more time to dry up due to their distance from the indoor climate [88] and the glue that connects the lamellas. In sum, the wood/timber surface treatment can have a significant influence on the drying capacity of section B, which will be heightened by a higher initial moisture content due, for example, to inappropriate material storage or unprotected construction site.

In addition, the risk for interstitial condensation was assessed in a specific location of the assembly, since its drying capacity decreases with the application of more impregnable surface wood treatments. The assessment was made by comparing the dew-point temperature against the temperature for the interface between the aluminium and the first spruce. If the obtained value is negative, it means that the temperature at the assessed location is higher than the respective dew-point temperature, which means that there is no risk of interstitial condensation. As it is shown in Fig. 8, all values for the five years are negative, which means no risk. However, it is also visible that there is a decrease of the difference in the first three years, but after that, for the first three assessed treatments, an increase of the difference occurs. While for the two more impregnable treatments there is still an increase afterwards. Nonetheless, it is observable that the five tested wood surface treatments do not lead to interstitial condensation risks.

3.3. Transient U-values

The transient U-values were calculated following the methodology described in subsection 2.4.2 using equation 4 that considers the variability of the U-value in accordance with moisture content in the assembly and the variability of the exterior heat resistance in accordance with wind. However, firstly, the moisture content (w, kg/m^3) for the hygroscopic materials – spruce 1–4 – that vary with time is shown in Fig. 9a–c, as well as their respective individual transient thermal resistance (R-value, (m^{2}K)/W) in Fig. 9d–f to understand the transient U-values. All parameters are presented for both dry and wet initial conditions, i.e. 60 % and 80 %RH. The thermal conductivity of the polyisocyanurate material does not vary significantly.

The box plots are for the first and last year and the U-values were calculated for both dry and wet initial conditions, i.e. 60 % and 80 %RH, respectively (Fig. 10). The box limits correspond to the 25th percentile and the 75th percentile, while the red line corresponds to the median. The whiskers correspond to the limits without outlines, and the red crosses are the outliners. The transient U-value accounts for the thermal resistance of the hygroscopic and non-hygroscopic materials. The transient U-values for section A are not shown here because its variation due to moisture content is marginal.

In terms of moisture content (Fig. 9a–c), it is visible that, as time advances, the assembly manages to dry, independently of the selected initial conditions, i.e. either 60 %RH (dashed lines) or 80 % RH (solid lines). However, this drying occurs at different speeds. It is faster the closer to the indoor climate (spruce 4) and slower the furthest to the indoor climate (spruce 1). This is even more evident when observing the assembly in wet conditions, i.e. 80 % RH (solid lines).

Since spruce 1 has at its left side, a non-hygroscopic material (i.e. aluminium frame, Fig. 2), then the only way to dry the excess of moisture is the indoor climate. However, it has to go across several other spruce layers (Fig. 2d). In addition, moisture is transported when there is a differential of relative humidity [89], so first the relative humidity has to decrease in the outer spruces, i.e. spruce 4, then spruce 3, and so forth, caused by the moisture exchanges with the indoor climate, which will eventually lead to its sequential drying. Only then, will the inner spruces be able to dry through a slow process, i.e. spruce 1 being the worst case. The difference between the analysed climates – i.e. Oslo, Trondheim and Tromsø – is not significant (Fig. 9a–c).

In terms of individual transient thermal resistance (Fig. 9d–f), the contrary behaviour is observed, i.e. the thermal resistance increases with time, which is understandable since the hygroscopic materials are able to dry (Fig. 9a–c). Hence, the moisture that saturated the material pores is gradually replaced by air, which has a much lower thermal conductivity than moisture [52] and, therefore, leads to the increase of the thermal resistance. Due to the drying behaviour previously explained, the highest values are firstly attained by spruce 4 in dry conditions, but gradually followed by the other spruces at different paces (Fig. 9d–f). Here, the difference between the analysed climates – i.e. Oslo, Trondheim and Tromsø – is also not significant (Fig. 9d–f).

For normal conditions, it is visible that by comparing the results between the first and last year for any of the selected climates, there is a slight reduction of the U-value (Fig. 10a–c). This is understandable since

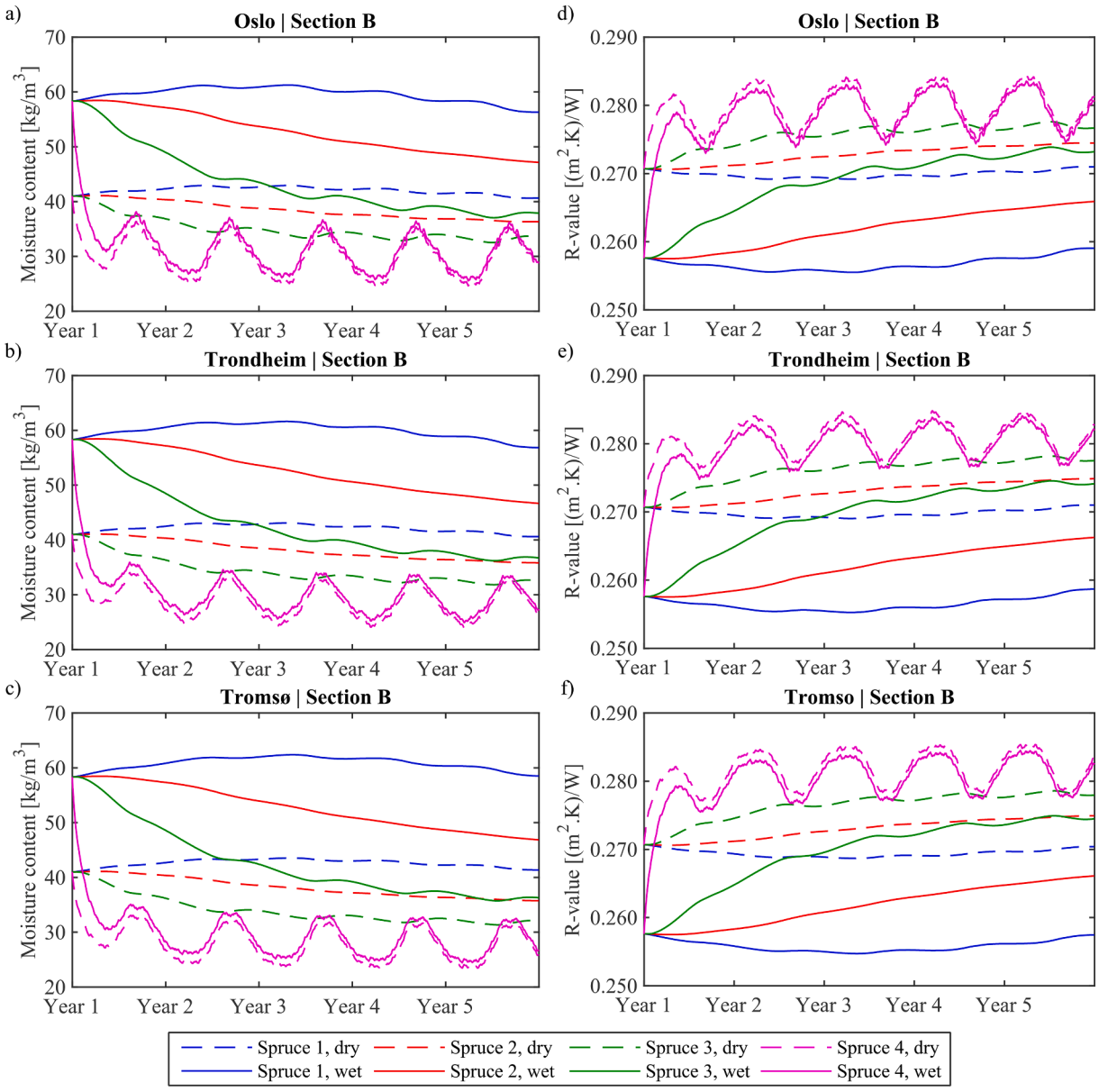

Fig. 9. Moisture content (kg/m^3) and thermal resistance ((m^{2}K)/W) for the five simulated years in the hygroscopic materials for Oslo (a and d), Trondheim (b and e) and Tromsø (c and f) for section B.

the moisture that exists within the lamellas at the beginning of the simulation will dry, so the porous media will be filled by air instead, which has a lower thermal conductivity than moisture [52] and, therefore, this leads to a lower U-value. However, the reduction is slight because the initial moisture content is for dry conditions, i.e. 60 %RH, and due to the facade system exterior (e.g. aluminium layer) and interior surface (e.g. wood surface treatment), moisture that comes from the exterior climate (e.g. wind-driven rain, which can be responsible for large amounts of moisture in walls [36]) and from the interior climate (e.g. moisture due to human activities [79]) is prevented from penetrating into the facade.

The polyisocyanurate insulation has the capacity to store moisture under normal conditions, and, therefore, its thermal conductivity is moisture dependent [26], but because of the fact that it is limited in both sides by aluminium, which is a very moisture impregnable material (i.e. low porosity, Table 1), then this hygroscopic layer is not in contact with moisture and, therefore, does not contribute to the variance of the transient U-value. The variance of the transient U-value is only caused by the variance of the spruce lamellas' moisture content and the exterior heat resistance, which is wind dependent [26].

It is also visible that there is a difference between having the material in dry state or in wet state for any of the simulated climates (Fig. 10a–c). Of course, this difference is more substantial for the first years because the amount of moisture is higher in the lamellas (Fig. 9a–c) and, therefore, their thermal conductivity is higher, which leads to higher U-values, and, therefore, greater energy losses. Note that if the simulations were to continue running the moisture content of each lamella would reach the values for their respective case with dry materials.

Nonetheless, it is safe to assume that the variance of the U-value due to moisture in the system, for any of the simulated cases, is not substantial, reaching, at most, 0.9 % for Oslo. In addition, the difference caused by having a higher initial moisture content is higher, but it is still not substantial, reaching, at most, 4.4 % for Tromsø. Note that these values also account for the influence of the surface heat resistance in accordance with the wind patterns.

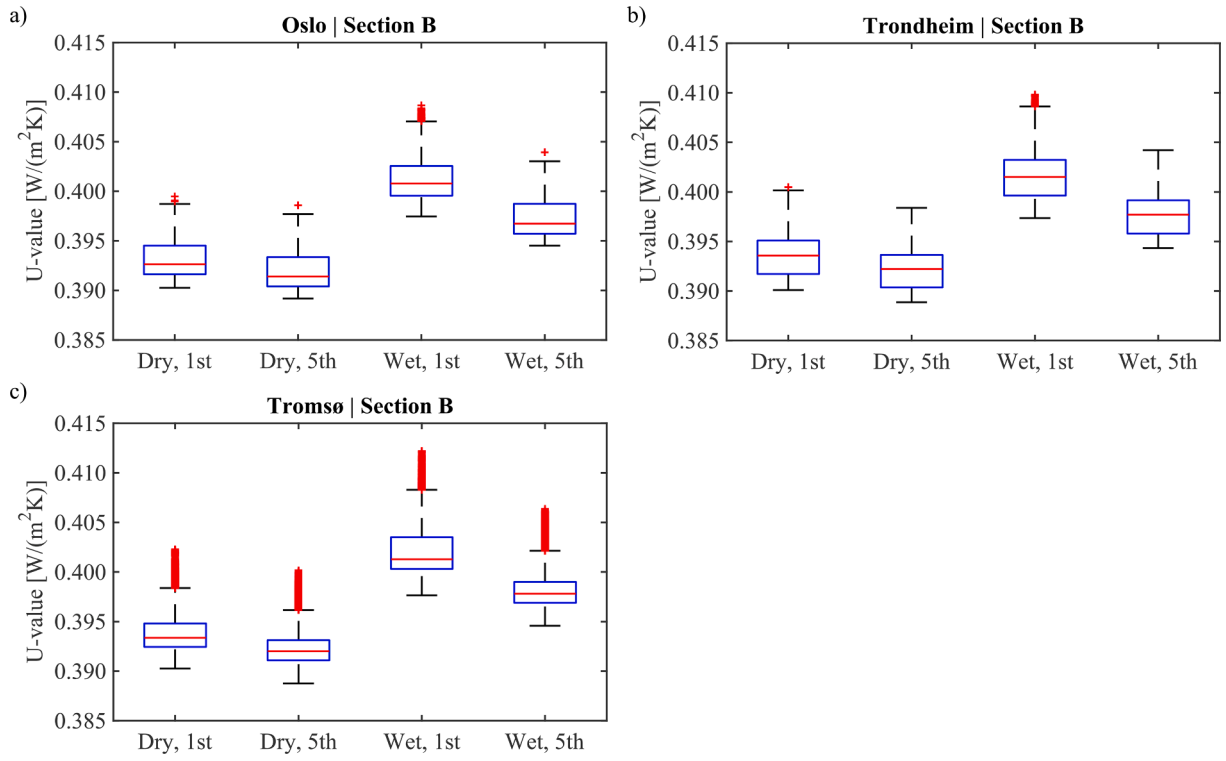

Fig. 10. U-value (W/(m^{2}K)) box plot for the first and last year of simulation for Oslo (a), Trondheim (b) and Tromsø (c) for section B.

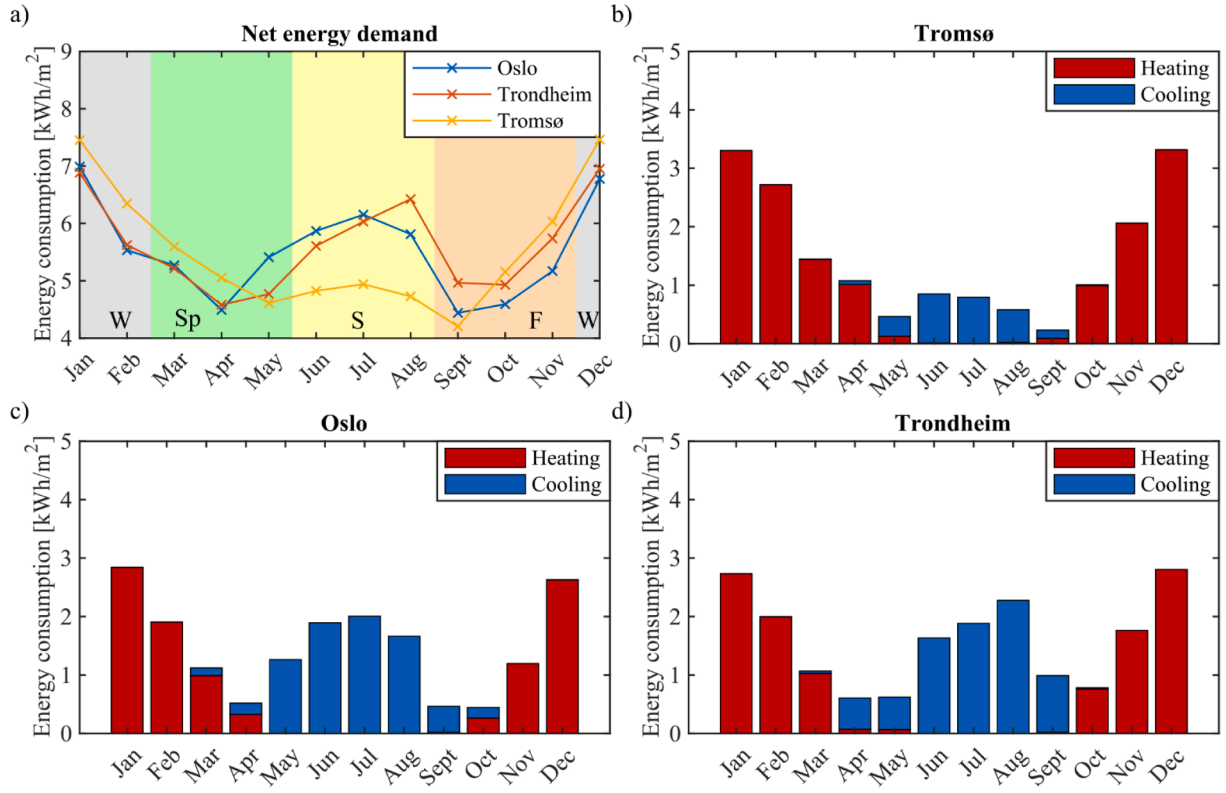

Fig. 11. Total net energy demand – heating, cooling, hot water, technical equipment, lighting – for each of the locations (a) and energy consumption due to heating needs (when $T_{int} < 21$ °C) and cooling needs (when T_{int} greater than 24 °C) for Tromsø (b), Oslo (c) and Trondheim (d). W corresponds to Winter, Sp corresponds to Spring, S corresponds to Summer and F corresponds to Fall.

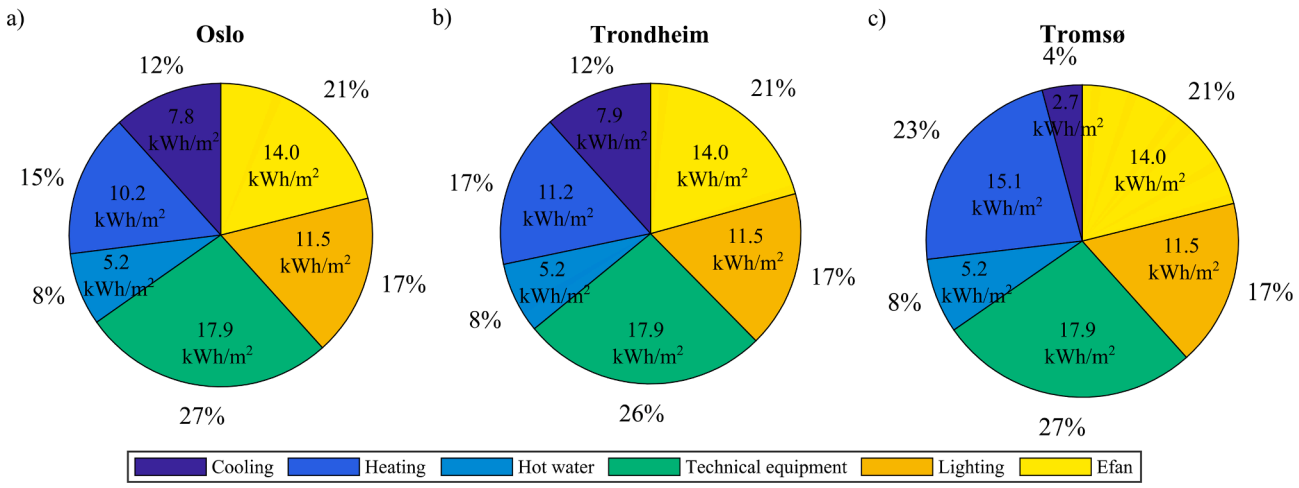

Fig. 12. Net energy demand (kWh/m^2) distribution – Cooling, heating, hot water, technical equipment, lighting and Efan – for Oslo (a), Trondheim (b) and Tromsø (c).

3.4. Net energy demand assessment

The net energy demand was assessed for each of the selected locations – Oslo, Trondheim and Tromsø (Fig. 11). The heating and cooling demands were obtained from the WUFI®Plus model in accordance with the setpoint strategy depicted in SN-NSPEK 3031 [55] for office buildings. The lighting energy demand of 42.6 Wh/m^2 per day, hot water energy demand of 19.2 Wh/m^2 per day, technical equipment energy demand of 66.6 Wh/m^2 per day, and fans energy demand were determined following methodology described in the SN-NSPEK 3031 [55] for office buildings. These energy demands, which are obtained from day-profiles, are building typology dependent, but they are not location dependent, which explains why they do not differ.

A specific fan power (SFP) of 1.5 kW/(m^3/s) was admitted [43]. The respective energy demand was calculated in accordance with the air volume set by SN-NSPEK 3031 [55] for offices. Although the daily sum of the energy consumption of hot water, technical equipment and lighting does not vary [55], the number of days in each month differs. This means that there is a marginal difference between months: 1) ca. 4.1 kWh/m^2 for the months that amount to 31 days – i.e. January, March, May, July, August, October and December; 2) ca. 3.9 kWh/m^2 for the months that amount to 30 days – i.e. April, June, September, November; and 3) ca. 3.6 kWh/m^2 for February (no leap-years).

Fig. 11a shows that the climate with the highest energy demand varies throughout the year. While in the Winter, the climate that has the highest demand is Tromsø due to the higher heating demands (Fig. 11b), which spreads to the first half of spring and the second half of Fall. During the remaining of the year, the energy demand is governed by the cooling demand with Oslo having the highest values until half of the Summer (Fig. 11c), which is then surpassed by Trondheim until half of Fall (Fig. 11d). This is easily understood by the outdoor temperature of the three climates, which shows that Tromsø has the lowest outdoor temperature almost all year around, while the warmest climate changes during the hotter months (Fig. A2).

The heating demand corresponds to 15, 17 and 23 % (Fig. 12) and the cooling demand corresponds to 12, 12 and 4 % (Fig. 12) of the yearly sum for Oslo, Trondheim and Tromsø, respectively. These are rather low values that are understandable due to the extremely low thermal transmittance of the different sections of the opaque wall (Table 1) and of the window system (i.e. 0.5 W/m^{2}K), which means that the room loses a low amount of energy through the exterior envelope and that is why the energy demand is similar for the three selected locations. The highest energy demand corresponds to the technical equipment (17.9 kWh/m^2), which is closely followed by Efan (14 kWh/m^2) and then by the lighting system (11.5 kWh/m^2). The lowest energy demand corresponds to the hot water (5.2 kWh/m^2). These four sources of energy demand amass to 73 % of the yearly sum.

In relation with the TEK17 limit value, i.e. 115 kWh/m^2 [43], the simulated case-study does not surpass this value for the three tested climates, i.e. Oslo, Trondheim and Tromsø. In fact, there is a comfortable margin of at least 41 % in relation to the limit value. While the six sources of energy demand amass to a value of 66.5 kWh/m^2 for Oslo, the yearly value for Trondheim and Tromsø is only slightly different, i.e. 66.4 and 67.7 kWh/m^2, respectively. These values are quite close because the four previously mentioned sources of energy demand have the same values, independently of the building's location. On the other hand, the heating and cooling demand vary, but to a minor extent, in which compensates each other variance, due to the key energy performance of the exterior envelope.

Nonetheless, the performance of the HUF system here simulated can be optimized in terms of its radiation behaviour of the HUF transparent section, e.g. optimize the windows' shading devices or films to take a more adequate advantage of the solar gains [92]. In the future, an advanced and complete energy assessment will be performed using a more energy-oriented software to account for a more complete heating/cooling system and mechanical ventilation system, like IDA ICE [93], since the assessments here presented were performed assuming an ideal system.

4. Conclusions

This paper describes a multistep approach for the hygrothermal assessment of a hybrid timber and aluminium based facade system, which is based on the use of WUFI®Pro and WUFI®Plus software. The WUFI®Plus model of a generic office building was built, using the hybrid facade system, to obtain the indoor conditions. Then, these conditions were used by the WUFI®Pro to thoroughly assess the hygrothermal performance of the facade sections in terms of mould growth and transient U-value, as well as to determine the influence of wood surface treatment for section B. The energy demand to guarantee the indoor temperature setpoint strategy defined by NSPEK 3031 was also assessed.

The analysis was carried out for three Norwegian cities, i.e. Oslo, Trondheim and Tromsø, to represent different climate zones in Norway. These weather files were built in accordance with the methodology described by ISO 15927–4 and the data was downloaded from the online database of the Norwegian Centre for Climate Services. As some gaps exist in the downloaded weather data, due to practical reasons, a user-independent code was developed to find these gaps and artificially fill them. This was found to be a very productive option, since it takes the

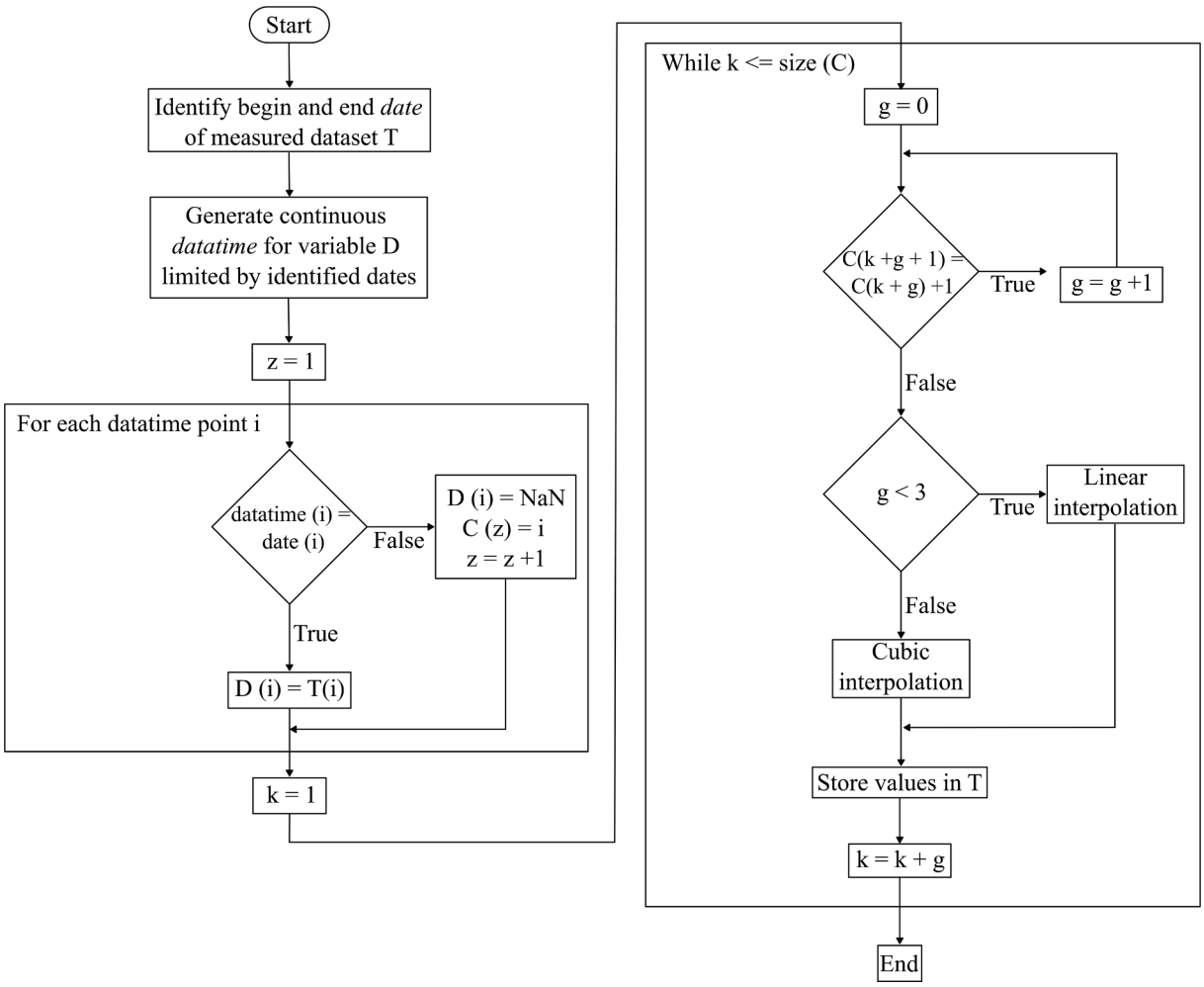

Fig. 13. Procedure to find the data gaps and artificially fill them in MATLAB.

code to check and fill the gaps of each 10-year batch, approximately 1.5 min for a total gap of 1849 h for batch 1 for temperature in Oslo.

The size of the gap influences the time taken by the code to run. In addition, it was concluded that the dataset should have no more than 10 % of gaps, but the lower the percentage of gaps, the better. In fact, it is not the total value of the gaps, but their individual size and their distribution, due to the used interpolation procedures basis, i.e. cubic interpolation, that can be limiting. For these cases, data from an alternative weather station or model/source should be used. It was seen that the errors associated with the artificial gap filling were minimized due to the construction of the reference year for the outdoor weather file.

It was shown that, under normal conditions, the hybrid facade system works properly in terms of moisture drying capacity. It does not allow moisture to penetrate, due to its composition, hence, there is no risk of mould growth. On the other hand, problems will arise if a higher initial moisture content exists within the building materials due, for example, to unprotected storage. Finally, it was also shown the great influence of the wood surface treatment can have on the drying capacity of the system.

In terms of mould growth, it was shown that for both simulated sections, there is no risk of mould growth since the mould index never overcomes the safety limit. In fact, it is far from it since the worst-case scenario occurs in Oslo with a mould index of 0.88 and the safety limit is 2.0. On contrary, if the building materials have a higher initial moisture content, the results are quite different. This safety limit is overcome for section A in the three climates before the first simulation year ends, attaining maximum values of 4.0, which means that the mould already covers more than 10 %. The situation is even worse for section B in which, contrary to section A, it never drops below the safety limit within the simulated period for any of the three climates. Tromsø even attains a maximum mould index of 6.0, which corresponds to a tight coverage, but it is closely followed by the other two climates. These results show the key importance of protecting these materials.

It was shown that the wood surface treatment can have a significant influence on the drying capacity of section B. This is especially true the closer the spruce lamella is to the indoor climate with the maximum moisture content difference between the wood surface treatment with 0.5 and 10.0 m reaching ca. 20 kg/m^3. For the inner lamellas, the difference caused by a moisture tighter wood surface treatment is only noticeable down a few years, due to their distance from the indoor climate, but also because of the glue that connects the lamellas.

It was shown that the climate with the highest energy demand varies throughout the year. While in the Winter, the climate that has the highest demand is Tromsø due to the higher heating demands, which spreads to the first half of Spring and the second half of Fall. During the remaining of the year, the energy demand is governed by the cooling demand with Oslo having the highest values until half of the Summer, which is then surpassed by Trondheim until half of Fall. The simulated case-study respects the TEK17 limit value for the three developed climates. Finally, it is safe to say that the variance of the U-value due to moisture in the system, for any of the simulated cases, is not substantial.

Through the developed methodology, the assembly was tested prior to its application in three different locations in Norway by means of using real measured meteorological conditions. It was possible to check

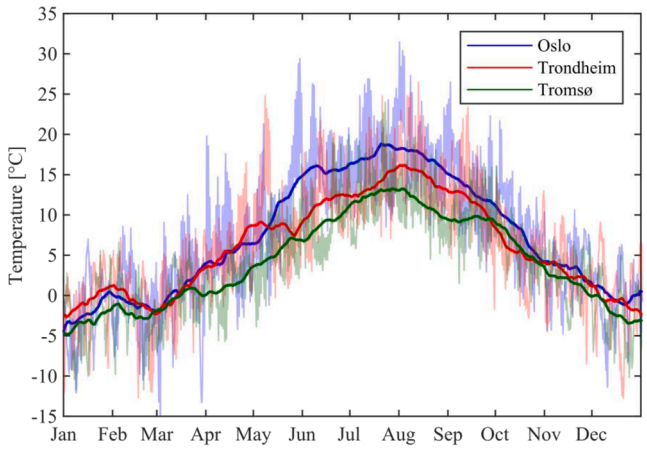

Fig. 14. Outdoor temperature in hourly values (thin lines) and monthly mean averages (bold lines) for Oslo, Trondheim and Tromsø.

that under normal conditions, there is no risk of mould growth for the tested assumptions. In addition, it was also possible to check the key importance of properly storing and transporting the building materials. Secondly, it was possible to observe the influence of the interior wood surface treatment on the drying capacity of the assembly, which does not lead to risk of interstitial condensation. Thirdly, it was shown that the assembly does not overcome the legal Norwegian limits in terms of net energy demand. Finally, this study presents a good example of applicability of the developed methodology by means of assessing and testing assemblies prior to their application, so that they can be optimized to withstand the particularities of where they are going to be installed.

This methodology is quite flexible since it can be replicated for any type of buildings and wall sections, as well as for other climate files given that the weather data is accessible or using already built climate files. It would be extremely advantageous to fully automatize the methodology to increase its time efficiency and lessen its error probability, but also to be able to perform sensitivity analysis or optimization studies in accordance with the study specifications autonomously. In addition, by incorporating in the future the development of the building geometry in BIM software, while assisted by 3D laser scanning, this would also allow to apply this fast and flexible methodology to already built buildings to assess their hygrothermal conditions in terms of e.g. mould risk.

CRediT authorship contribution statement

Guilherme B.A. Coelho: Conceptualization, Methodology, Software, Validation, Formal analysis, Investigation, Writing – original draft, Visualization. **Dimitrios Kraniotis:** Conceptualization, Methodology, Validation, Resources, Writing – review & editing, Funding acquisition.

Declaration of Competing Interest

The authors declare that they have no known competing financial interests or personal relationships that could have appeared to influence the work reported in this paper.

Data availability

Data will be made available on request.

Acknowledgments

The authors acknowledge the EEA and Norway grants for the financial support through project LT07-1-EIM-K01-003 (“*Development of a less polluting, automated façade system integrated into building management systems*”). The authors also acknowledge Rita de Vasconcelos (oficina’lx) for her help designing the methodology scheme. Fig. 4 was reprinted from Lisø KR, Kvande T., Klimatilpasning av bygninger (Klima2000), Copyright (2007), with permission from SINTEF Byggforsk 2007.

Appendix

Figs. A1 and A2

References

[1] Directive 2010/31/EU of the European Parliament and of the Council of 19 May 2010 on the energy performance of buildings, L153/13, Official Journal of the European Union. (2010).
[2] OECD stat, Greenhouse gas emissions, https://stats.oecd.org/Index.aspx?DataSetCode=AIR_GHG# (accessed January 2023).
[3] StaticusCare project - website, https://staticuscare.com/ (accessed October 2022).
[4] S. Pastori, E. Sergio Mazzucchelli, M. Wallhagen, Hybrid timber-based structures: a state of the art review, Constr. Build. Mater. 359 (2022), 129505, https://doi.org/10.1016/j.conbuildmat.2022.129505.
[5] A. Ahmed, J. Sturges, Materials Science in Construction: An Introduction, Routledge, 2015.
[6] V. Bucur, Acoustics of Wood, 2nd Edition, Springer-Verlag Berlin Heidelberg, 206AD.
[7] K. Nore, A.Q. Nyrud, D. Kraniotis, K.R. Skulberg, F. Englund, T. Aurlien, Moisture buffering, energy potential, and volatile organic compound emissions of wood exposed to indoor environments, Science and Technology for the Built Environment. 23 (2017) 512–521, https://doi.org/10.1080/23744731.2017.1288503.
[8] D. Kraniotis, K. Nore, Latent Heat Phenomena in Buildings and Potential Integration into Energy Balance, Procedia Environ. Sci. 38 (2017) 364–371, https://doi.org/10.1016/j.proenv.2017.03.102.
[9] D. Kraniotis, K. Nore, C. Brückner, A.Q. Nyrud, Thermography measurements and latent heat documentation of Norwegian spruce (Picea abies) exposed to dynamic indoor climate, J. Wood Sci. 62 (2016) 203–209, https://doi.org/10.1007/s10086-015-1528-1.
[10] C. Rode, R. Peuhkuri, B. Time, K. Svennberg, T. Ojanen, P. Mukhopadhyaya, M. Kumaran, S.W. Dean, Moisture Buffer Value of Building Materials, J. ASTM Int. 4 (5) (2007) 100369.
[11] Z. Pasztory, P.N. Peralta, S. Molnar, I. Peszlen, Modeling the hygrothermal performance of selected North American and comparable European wood-frame house walls, Energ. Buildings 49 (2012) 142–147, https://doi.org/10.1016/j.enbuild.2012.02.003.
[12] E. Gasparri, M. Aitchison, Unitised timber envelopes. A novel approach to the design of prefabricated mass timber envelopes for multi-storey buildings, Journal of Building Engineering. 26 (2019), 100898, https://doi.org/10.1016/j.jobe.2019.100898.
[13] K.R. Lisø, T. Kvande, Klimatilpasning av bygninger (Klima2000), SINTEF (2007).
[14] K. Gradeci, N. Labonnote, B. Time, J. Köhler, A proposed probabilistic-based design methodology for predicting mould occurrence in timber façades. In: WCTE 2016 - World Conference on Timber Engineering, 2016.
[15] T.K. Thiis, I. Burud, D. Kraniotis, L.R. Gobakken, The role of transient wetting on mould growth on wooden claddings, Energy Procedia 78 (2015) 249–254, https://doi.org/10.1016/j.egypro.2015.11.629.
[16] T.K. Thiis, I. Burud, A. Flø, D. Kraniotis, S. Charisi, P. Stefansson, Monitoring and simulation of diurnal surface conditions of a wooden façade, Procedia Environ. Sci. 38 (2017) 331–339, https://doi.org/10.1016/j.proenv.2017.03.088.
[17] K. Gradeci, U. Berardi, B. Time, J. Köhler, Evaluating highly insulated walls to withstand biodeterioration: A probabilistic-based methodology, Energ. Buildings 177 (2018) 112–124, https://doi.org/10.1016/j.enbuild.2018.07.059.
[18] K. Sedlbauer, Prediction of mould fungus formation on the surface of and inside building components, Fraunhofer Institute for Building Physics, 2001. PhD thesis.
[19] K. Gradeci, N. Labonnote, B. Time, J. Köhler, Mould growth criteria and design avoidance approaches in wood-based materials – A systematic review, Constr. Build. Mater. 150 (2017) 77–88, https://doi.org/10.1016/j.conbuildmat.2017.05.204.
[20] WHO guidelines for indoor air quality: dampness and mould, (2009).
[21] V. Cascione, E. Marra, D. Zirkelbach, S. Liuzzi, P. Stefanizzi, Hygrothermal analysis of technical solutions for insulating the opaque building envelope, Energy Procedia 126 (2017) 203–210, https://doi.org/10.1016/j.egypro.2017.08.141.
[22] N.M.M. Ramos, E. Barreira, M.L. Simões, J.M.P.Q. Delgado, Probabilistic risk assessment methodology of exterior surfaces defacement caused by algae growth, J. Constr. Eng. Manag. 140 (2014) 1–8, https://doi.org/10.1061/(asce)co.1943-7862.0000909.
[23] R.M.S.F. Almeida, E. Barreira, Monte carlo simulation to evaluate mould growth in walls: the effect of insulation, orientation, and finishing coating, Advances in Civil Engineering. 2018 (2018) 1–12.
[24] M. Zhao, H.M. Künzel, S.R. Mehra, Design hygrothermally functional wooden insulation systems: a parametric study for mixed climate, J. Build. Phys. 46 (2023) 474–509, https://doi.org/10.1177/17442591221142506.

[25] A.D. Trindade, G.B.A. Coelho, F.M.A. Henriques, Influence of the climatic conditions on the hygrothermal performance of autoclaved aerated concrete masonry walls, Journal of Building Engineering. 33 (2021) 101578.
[26] WUFI®Pro, Moisture design tool for architects and engineers, Version 5.3, Fraunhofer Institute for Building Physics (Fraunhofer IBP).
[27] WUFI®Plus, Version 3.1.1.0, Fraunhofer Institute for Building Physics (Fraunhofer IBP), (2017).
[28] WUFI-Bio, Assessing the Risk of Mould Growth, Version 4.0, Fraunhofer Institute for Building Physics (Fraunhofer IBP).
[29] P. Choidis, D. Kraniotis, I. Lehtonen, B. Hellum, A modelling approach for the assessment of climate change impact on the fungal colonization of historic timber structures, Forests 12 (2021) 819, https://doi.org/10.3390/f12070819.
[30] G.B.A. Coelho, V.P. de Freitas, F.M.A. Henriques, H.E. Silva, Retrofitting historic buildings for future climatic conditions and consequences in terms of artifacts conservation using hygrothermal building simulation, Appl. Sci. 13 (2023) 2382, https://doi.org/10.3390/app13042382.
[31] Meteonorm 8 - Global Meteorological Database, Meteotest AG, (2020).
[32] CBE Clima Tool, https://clima.cbe.berkeley.edu/ (accessed March 2023).
[33] G.B.A. Coelho, H.E. Silva, F.M.A. Henriques, Calibrated hygrothermal simulation models for historical buildings, Build. Environ. 142 (2018) 439–450, https://doi.org/10.1016/j.buildenv.2018.06.034.
[34] WMO, Calculation of monthly and annual 30-year standard normals. WCDP 10 and WMOTD 341, World Meteorological Organization, Meeting of Experts. (1989) 14.
[35] J. Zhang, L. Pezoulas, K. Karagiozis, Environmental Weather Loads for Hygrothermal Analysis and Design of Buildings (ASHRAE RP-1325), (2011).
[36] G.B.A. Coelho, F.M.A. Henriques, Influence of driving rain on the hygrothermal behavior of solid brick walls, Journal of Building Engineering. 7 (2016) 121–132, https://doi.org/10.1016/j.jobe.2016.06.002.
[37] E.N. ISO, 15927–4, Hygrothermal performance of buildings - Calculation and presentation of climatic data - Part 4: Hourly data for assessing the annual energy use for heating and cooling, European Commitee for Standardization (CEN) (2005) 16.
[38] M. Salonvaara, RP-1325, Environmental weather loads for hygrothermal analysis and design of buildings, (2011) 96.
[39] EnergyPlus, Input Output Reference, Bigladder Software. (2015) 2109. http://bigladdersoftware.com/epx/docs/8-3/input-output-reference/index.html.
[40] G.B.A. Coelho, F.M.A. Henriques, Performance of passive retrofit measures for historic buildings that house artefacts viable for future conditions, Sustain. Cities Soc. 71 (2021), 102982, https://doi.org/10.1016/j.scs.2021.102982.
[41] Norwegian Centre For Climate Services, https://klimaservicesenter.no/ (accessed in October 2022).
[42] S. Geving, S.E. Torgersen, Klimadata for fuktberegninger. Referanseår for 12 steder i Norge og klimadata for konstruksjoner mot grunnen (Prosjektrapport 227), (1997).
[43] Byggteknisk forskrift (TEK17) med veiledning, https://dibk.no/regelverk/byggteknisk-forskrift-tek17/14/14-2/ (accessed January 2023).
[44] E.N. ISO, 13788:2012 Hygrothermal performance of building components and building elements - internal surface temperature to avoid critical surface humidity and interstitial condensation Calculation methods, European Committee for Standardization (CEN) (2012).
[45] G.B.A. Coelho, D. Kraniotis, Numerical investigation of mould growth risk in a timber-based facade system under current and future climate scenarios, in: Nordic Symposium on Building Physics (NSB 2023), 2023.
[46] G.B.A. Coelho, H.E. Silva, F.M.A. Henriques, Impact of climate change in cultural heritage: from energy consumption to artefacts' conservation and building rehabilitation, Energ. Buildings 224 (2020), 110250, https://doi.org/10.1016/j.enbuild.2020.110250.
[47] World Meteorology Organization (WMO), Guide to Meteorological Instruments and Methods of observation (WMO-No.8), 2014.
[48] J.C. Baltazar-Cervantes, D.E. Claridge, Restoration of short periods of missing energy use and weather data using cubic spline and fourier series approaches: qualitative analysis, in: Proceedings of the 13th Symposium on Improving Building Systems in Hot and Humid Climates, 2002, pp. 213–218.
[49] G.B.A. Coelho, F.M.A. Henriques, The importance of moisture transport properties of wall finishings on the hygrothermal performance of masonry walls for current and future climates, Appl. Sci. 13 (2023) 6318, https://doi.org/10.3390/app13106318.
[50] A. Karagiozis, H.M. Künzel, A. Holm, WUFI ORNL/IBP–A North American Hygrothermal Model, in: Proceedings of the Thermal Performance of the Exterior Envelopes of Whole Buildings VIII, Clearwater Beach, Florida, USA, 2001.
[51] J.M.P.Q. Delgado, N.M.M. Ramos, E. Barreira, V.P. de Freitas, A critical review of hygrothermal models used in porous building materials, Journal of Porous Media. 13 (2010) 221–234, https://doi.org/10.1615/jpormedia.v13.i3.30.
[52] E.N. ISO, 10456:2007, Building materials and products - Hygrothermal properties -Tabulated design values and procedures for determining declared and design thermal values, European Committee for Standardization (CEN), 2007.
[53] Materialer til luft- og damptetting (573.121), (2003) 1–6.
[54] Staticus,, Hybrid Unitized Façade (HUF) - Highly sustainable building envelope, Project kickoff presentation (2022).
[55] SN-NSPEK,, 3031:2021, Bygningers energiytelse energiforsyning (Energy performance of buildings Calculation of energy needs and energy supply), Norsk Spesifikasjon (2021).
[56] WUFI wiki - Climate Data, https://www.wufi-wiki.com/mediawiki/index.php/Details:Climate (accessed October 2022).
[57] World Meteorological Organization, Guide to Climatological Practices WMO-No. 100, 2011. https://doi.org/WMO-No. 100.
[58] E. Barreira, J.M.P.Q. Delgado, N.M.M. Ramos, V.P. de Freitas, Exterior condensations on façades: numerical simulation of the undercooling phenomenon, J. Build. Perform. Simul. 6 (2013) 337–345, https://doi.org/10.1080/19401493.2011.560685.
[59] G. Pelletier, solrad.xls (version 1.2) - A solar position and radiation calculator for Microsoft Excel/VBA.
[60] R.E. Bird, R. Hulstrom, A Simplified Clear Sky model for Direct and Diffuse Insolation on Horizontal Surfaces, SERI Technical Report SERI/TR-642-761 (1991).
[61] R.R. Perez, P. Ineichen, E.L. Maxwell, R.D. Seals, A. Zelenka, Dynamic global-to-direct irradiance conversion models, ASHRAE Trans. 98 (1992) 354–369.
[62] R. Perez, P. Ineichen, R. Seals, A. Zelenka, Making full use of the clearness index for parameterizing hourly insolation conditions, Sol. Energy 45 (1990) 111–114, https://doi.org/10.1016/0038-092X(90)90036-C.
[63] E.L. Maxwell, A quasi-physical model for converting hourly Global Horizontal to Direct Normal Insolation, Solar Energy Research Institute. (1987) 35–46. http://rredc.nrel.gov/solar/pubs/PDFs/TR-215-3087.pdf.
[64] J. Wright, R. Perez, J.J. Michalsky, Luminous efficacy of direct irradiance: Variations with insulation and moisture conditions, Sol. Energy 42 (1988) 387–394.
[65] M. Iqbal, An Introduction to Solar Radiation, Academic Press, 1983.
[66] M. Mikofski, Solar Position Calculator, https://www.mathworks.com/matlabcentral/fileexchange/58405-solar-position-calculator?s_tid=prof_contriblnk (accessed June 2019).
[67] G.B.A. Coelho, Optimization of historic buildings that house artefacts considering climate change, FCT-UNL, 2020. PhD Thesis),.
[68] NOAA ESRL - Solar Geometry Calculator, https://www.esrl.noaa.gov/gmd/grad/antuv/SolarCalc.jsp (accessed June 2019).
[69] F. Kasten, A.T. Young, Revised optical air mass tables and approximation formula, Appl. Opt. 28 (1989) 4735–4738.
[70] DIN 4108-3, Wärmeschutz und Energie-Einsparung in Gebäuden - Teil 3: Klimabedingter Feuchteschutz - Anforderungen, Berechnungsverfahren und Hinweise für Planung und Ausführung, Deutsches Institut für Normung (DIN), (2012).
[71] VDI 3789:2001 - Umweltmeteorologie Wechselwirkungen zwischen Atmosphäre und Oberflächen Berechnung der spektralen Bestrahlungsstärken im solaren Wellenlängenbereich, Verein Deutscher Ingenieure (VDI), (2001).
[72] NREL - DISC model (excel), https://www.nrel.gov/grid/solar-resource/disc.html (accessed January 2023).
[73] Source code for pvlib.irradiance, https://pvlib-python.readthedocs.io/en/v0.7.1/_modules/pvlib/irradiance.html#perez (accessed February 2023).
[74] Meteonorm Handbook part II: Theory. Global Meteorological Database (Version 8), https://meteonorm.com/assets/downloads/mn80_software.pdf.
[75] T.E. Skaugen, O.E. Tveito, Heating degree-days – Present conditions and scenario for the period 2021–2050, Norwegian Meteorological Institute, 2002.
[76] Climate change 2014, Impacts, adaptation, and vulnerability Part B: Regional aspects: Working group II contribution to the fifth assessment report of the intergovernmental panel on climate change [Barros, V.R., C.B. Field, D.J. Dokken, M.D. Mastrandrea, K, (n.d.) 688.
[77] ISO 7730:2005, Ergonomics of the thermal environment - Analytical determination and interpretation of thermal comfort using calculation of the PMV and PPD indices and local thermal comfort criteria, International Organization for Standardization (ISO), (2005).
[78] U.S. Department of Energy, Input Output Reference (version 8.8.0), (2017) 1–2657.
[79] American Society of Heating Refrigerating and Air-Conditioning Engineers (ASHRAE), ASHRAE Handbook - Fundamentals, Atlanta, USA, 2013.
[80] S. Hameury, Moisture buffering capacity of heavy timber structures directly exposed to an indoor climate: a numerical study, Build. Environ. 40 (2005) 1400–1412, https://doi.org/10.1016/j.buildenv.2004.10.017.
[81] ASTM 6245:2012, Standard Guide for Using Indoor Carbon Dioxide Concentrations to Evaluate Indoor Air Quality and Ventilation, American Society for Testing and Materials (ASTM), (2012). https://doi.org/10.1520/D6245-12.Copyright.
[82] Isothermal Properties for Carbon dioxide, NIST Chemistry WebBook, SRD 69, https://webbook.nist.gov/cgi/fluid.cgi?T=20&PLow=0.95&PHigh=1.05&PInc=0.05&Digits=5&ID=C124389&Action=Load&Type=IsoTherm&TUnit=C&PUnit=atm&DUnit=kg%2Fm3&HUnit=kJ%2Fmol&WUnit=m%2Fs&V.
[83] A. Brambilla, A. Sangiorgio, Mould growth in energy efficient buildings: Causes, health implications and strategies to mitigate the risk, Renew. Sustain. Energy Rev. 132 (2020), 110093, https://doi.org/10.1016/j.rser.2020.110093.
[84] H. Viitanen, M. Krus, T. Ojanen, V. Eitner, D. Zirkelbach, Mold risk classification based on comparative evaluation of two established growth models, Energy Procedia 78 (2015) 1425–1430, https://doi.org/10.1016/j.egypro.2015.11.165.
[85] A. Hukka, H. Viitanen, A mathematical model of mould growth on wooden material, Wood Sci. Technol. 33 (1999) 475–485, https://doi.org/10.1007/s002260050131.
[86] H. Viitanen, A. Ritschkoff, Mold growth in pine and spruce sapwood in relatioon to air humidity and temperature, Swedish University of Agriculture Sciences, Department of Forrest Products, Uppsala, 1991.
[87] Y.A. Cengel, Heat Transfer: A Practical Approach, 2nd edi.,, Mcgraw-Hill, 2002.
[88] C. Hall, W.D. Hoff, Water Transport in Brick, Stone and Concrete, 2nd ed., Spon Press, London, England, 2012.
[89] H. Künzel, Simultaneous Heat and Moisture Transport in Building Components One-and two-dimensional calculation using simple parameters, Fraunhofer IRB Verlag Suttgart. (1995).

[90] M. Amorim, V.P. de Freitas, I. Torres, Influence of moisture on the energy performance of retrofitted walls - experimental assessment and validation of an hygrothermal model, Int. J. Archit. Herit. 00 (2023) 1–15, https://doi.org/10.1080/15583058.2022.2157777.
[91] Byggforskserien - Materialdata for vanndamptransport - 573.430, https://www.byggforsk.no/dokument/606/materialdata_for_vanndamptransport (accessed February, 2023).
[92] M. Rabani, H. Bayera Madessa, N. Nord, Achieving zero-energy building performance with thermal and visual comfort enhancement through optimization of fenestration, envelope, shading device, and energy supply system, Sustainable Energy Technol. Assess. 44 (2021), 101020, https://doi.org/10.1016/j.seta.2021.101020.
[93] IDA Indoor Climate and Energy (IDA ICE) - version 4.8 SP2, EQUA Simulation AB.